

**Online rheological characterization of highly filled  
polymer melts employed in powder injection moulding  
with the special regard to wall-slippage**

Bc. Soňa Mizeráková

---

Master thesis  
2013

 Tomas Bata University in Zlín  
Faculty of Technology

---

Univerzita Tomáše Bati ve Zlíně

Fakulta technologická

Ústav fyziky a mater. inženýrství

akademický rok: 2012/2013

## ZADÁNÍ DIPLOMOVÉ PRÁCE

(PROJEKTU, UMĚLECKÉHO DÍLA, UMĚLECKÉHO VÝKONU)

Jméno a příjmení: **Bc. Soňa Mizeráková**

Osobní číslo: **T11700**

Studijní program: **N2808 Chemie a technologie materiálů**

Studijní obor: **Materiálové inženýrství**

Forma studia: **prezenční**

Téma práce: **Reologické vlastnosti vysoce plněných polymerních tavenin se zaměřením na skluz na stěně měřené na online plastografu**

Zásady pro vypracování:

The aim of this master thesis is online rheological characterization of highly filled polymer melts employed in powder injection molding (PIM) with the special regard to wall-slip. Wall-slip is the rheological phenomenon which might serve as an indicator for phase separation of PIM compounds. The theoretical part describes specifics of rheological behavior of highly filled polymer melts, and also introduces PIM technology in general. The practical part deals with rheological testing of various commercially available feedstock compositions in online rheometer and SEM microscopy.

Rozsah diplomové práce:

Rozsah příloh:

Forma zpracování diplomové práce: **tištěná**

Seznam odborné literatury:

1. **BARNES, H. A.: A review of the slip (wall depletion) of polymer solutions, emulsions and particle suspensions in viscometers: its cause, character, and cure. Journal of Non-Newtonian Fluid Mechanics: p. 221 - 251 (1995)**
2. **HAUSNEROVÁ, B.: Powder Injection Moulding - An Alternative Processing Method for Automotive Items. Trends and Developments in Automotive Engineering, Vienna: InTech, p. 129-146 (2011).**

Vedoucí diplomové práce:

**prof. Ing. Berenika Hausnerová, Ph.D.**

Ústav výrobního inženýrství

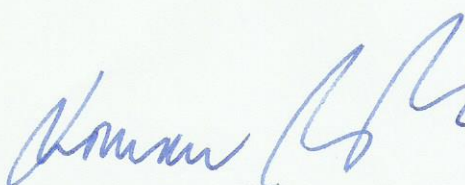
Datum zadání diplomové práce:

**8. února 2013**

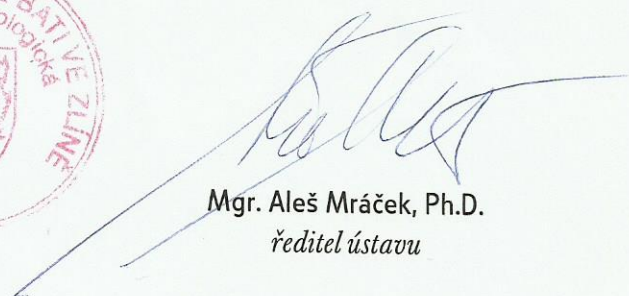
Termín odevzdání diplomové práce:

**24. května 2013**

Ve Zlíně dne 14. února 2013



doc. Ing. Roman Čermák, Ph.D.  
*děkan*



Mgr. Aleš Mráček, Ph.D.  
*ředitel ústavu*

## PROHLÁŠENÍ

Prohlašuji, že

- beru na vědomí, že odevzdáním diplomové/bakalářské práce souhlasím se zveřejněním své práce podle zákona č. 111/1998 Sb. o vysokých školách a o změně a doplnění dalších zákonů (zákon o vysokých školách), ve znění pozdějších právních předpisů, bez ohledu na výsledek obhajoby<sup>1)</sup>;
- beru na vědomí, že diplomová/bakalářská práce bude uložena v elektronické podobě v univerzitním informačním systému dostupná k nahlédnutí, že jeden výtisk diplomové/bakalářské práce bude uložen na příslušném ústavu Fakulty technologické UTB ve Zlíně a jeden výtisk bude uložen u vedoucího práce;
- byl/a jsem seznámen/a s tím, že na moji diplomovou/bakalářskou práci se plně vztahuje zákon č. 121/2000 Sb. o právu autorském, o právech souvisejících s právem autorským a o změně některých zákonů (autorský zákon) ve znění pozdějších právních předpisů, zejm. § 35 odst. 3<sup>2)</sup>;
- beru na vědomí, že podle § 60<sup>3)</sup> odst. 1 autorského zákona má UTB ve Zlíně právo na uzavření licenční smlouvy o užití školního díla v rozsahu § 12 odst. 4 autorského zákona;
- beru na vědomí, že podle § 60<sup>3)</sup> odst. 2 a 3 mohu užit své dílo – diplomovou/bakalářskou práci nebo poskytnout licenci k jejímu využití jen s předchozím písemným souhlasem Univerzity Tomáše Bati ve Zlíně, která je oprávněna v takovém případě ode mne požadovat přiměřený příspěvek na úhradu nákladů, které byly Univerzitou Tomáše Bati ve Zlíně na vytvoření díla vynaloženy (až do jejich skutečné výše);
- beru na vědomí, že pokud bylo k vypracování diplomové/bakalářské práce využito softwaru poskytnutého Univerzitou Tomáše Bati ve Zlíně nebo jinými subjekty pouze ke studijním a výzkumným účelům (tedy pouze k nekomerčnímu využití), nelze výsledky diplomové/bakalářské práce využít ke komerčním účelům;
- beru na vědomí, že pokud je výstupem diplomové/bakalářské práce jakýkoliv softwarový produkt, považují se za součást práce rovněž i zdrojové kódy, popř. soubory, ze kterých se projekt skládá. Neodevzdání této součásti může být důvodem k neobhájení práce.

Ve Zlíně 21.05.2013



.....

## **ABSTRAKT**

Táto diplomová práca sa zaoberá skúmaním reologických vlastností počas spracovania vysoko plnených polymérnych tavenín pripravených PIM technológiou. Špeciálna pozornosť je venovaná sklzu na stene ako kvalitatívnemu parametru fázovej separácie, ktorá je nežiaducim javom počas spracovania takýchto materiálov a kritickým bodom pri plnení formy. Testované boli komerčne dostupné materiály (PolyMIM 17-4PH, PolyMIM 316L, Catamold 316L and Embemold 17-4PH), ktoré sa líšili buď v zložení kovového prášku, alebo polymérnej matrice. Získané vzorky boli vytlačované cez slit die hlavicu namontovanú na online reometry a ich štruktúra bola sledovaná pomocou skenovacej elektrónovej mikroskopie a povrchovej analýzy.

**Kľúčové slová:** vysoko plnené polymérne taveniny, online reometer, slit die, sklz na stene, PIM technológia, fázová separácia

## **ABSTRACT**

This master thesis deals with the rheological characterization and processing traits of highly filled polymer melts employed in powder injection moulding (PIM). The special emphasis is placed on the wall-slip phenomenon considered as a qualitative parameter indicating phase separation of PIM compounds, which is undesirable and critical processability point during the mould filling. Commercially available feedstocks (PolyMIM 17-4PH, PolyMIM 316L, Catamold 316L and Embemold 17-4PH) which differed either in metal powder or polymer binder composition were used for testing. The samples were extruded through the slit die head mounted on online rheometer and their structure was studied by means of SEM and surface analysis.

**Keywords:** highly filled polymer melts, online rheometer, slit die, wall-slip, PIM technology, phase separation

## **Acknowledgement**

I would like to thank all those people who have been very helpful to me during the measurements and writing of my master thesis, and whose support I really appreciate.

Firstly, I would like to thank my diploma advisor prof. Ing. Berenika Hausnerová, Ph.D. from Tomas Bata University for her guidance, help and support throughout this research and data evaluation.

Special thanks belong to Ing. Gordana Paravanová, Ph.D. and Ing. Lucia Čučová for their assistance with the rheological measurements, to Ing. Luboš Rokyta for the roughness measurements of slit die channel surfaces and to doc. Dr. Ing. Vladimír Pata for help with the surface scanning of extruded samples.

I would also like to thank to the Centre of Polymer Systems TBU in Zlin for providing of selected PIM feedstocks and all measuring equipments.

My deep acknowledgement is directed to my family and close friends for their continuous support during all my studies.

I hereby declare, that this master thesis was carried out independently and only by use of the aids that are stated. I further declare that the presented version of master thesis and the electronic one recorded to IS/STAG are identical.

Zlín, 6<sup>th</sup> May 2013

.....

Signature

# CONTENTS

<b>INTRODUCTION .....</b>	<b>9</b>
<b>I THEORETICAL PART .....</b>	<b>10</b>
<b>1 HIGHLY FILLED POLYMER MATERIALS .....</b>	<b>11</b>
1.1 POWDER INJECTION MOULDING .....	11
1.1.1 PIM feedstock preparation .....	13
1.1.2 Injection moulding .....	15
<b>2 RHEOLOGY OF HIGHLY FILLED SYSTEMS.....</b>	<b>16</b>
2.1 RHEOLOGICAL APPROACHES TO OPTIMIZE PIM PROCESS.....	16
2.1.1 Binder formulation .....	16
2.1.2 Determination of powder/binder ratio.....	18
2.1.3 A phase separation.....	20
<b>3 WALL DEPLETION EFFECT .....</b>	<b>23</b>
3.1 PHENOMENA THAT GIVE RISE TO WALL DEPLETION .....	24
3.2 A MANIFESTATIONS OF SLIP .....	24
3.3 APPROACHES TO ELIMINATING OF SLIP .....	27
3.4 SLIP IN PARTICULAR GEOMETRIES .....	29
3.4.1 Tubes .....	29
3.4.2 Cylinders .....	31
3.4.3 Parallel plates .....	32
<b>II EXPERIMENTAL PART .....</b>	<b>35</b>
<b>4 CHARACTERISTICS OF FEEDSTOCKS.....</b>	<b>36</b>
<b>5 TESTING METHODS.....</b>	<b>39</b>
5.1 CHANNEL SURFACE MEASUREMENTS.....	39
5.1.1 Surface roughness .....	39
5.2 RHEOLOGICAL MEASUREMENTS .....	39
5.2.1 Online rheometry .....	39
5.3 MORPHOLOGY MEASUREMENTS .....	40
5.3.1 Scanning electron microscopy (SEM) .....	40
5.3.2 Surface analysis.....	40
<b>6 RESULTS AND DISCUSSION .....</b>	<b>41</b>

6.1	MATERIALS .....	41
6.2	GEOMETRY SELECTION .....	42
6.3	SLIT DIE ROUGHNESS MEASUREMENTS .....	43
6.4	RHEOLOGY .....	46
6.5	STRUCTURE ANALYSES .....	58
	<b>CONCLUSION .....</b>	<b>64</b>
	<b>BIBLIOGRAPHY .....</b>	<b>66</b>
	<b>LIST OF ABBREVIATIONS .....</b>	<b>70</b>
	<b>LIST OF FIGURES .....</b>	<b>70</b>
	<b>LIST OF TABLES.....</b>	<b>75</b>



## INTRODUCTION

Highly filled suspensions, which are filled close to their maximum packing fraction, are processed widely in various industries. They include the batch and continuous compounding and shaping of thermoplastic and thermosetting resins, moulding of ceramic articles, and mixing of solid fuels (Yilmazer, Kalyon; 1989).

The rheological behaviour of concentrated suspensions has been the subject of several reviews. A detailed understanding of the rheology of highly filled systems is a prerequisite for their optimum and safe processing. Some of the important aspects of the rheological properties of highly filled suspensions involve mat formation and flow instabilities, slip effects and the shear induced migration of particles in concentrated solutions. In the flow of polymer melts, containing moderate concentrations of particulate fillers, migration effects increase with increasing shear stress (Kalyon, Yilmazer; 1989). Recently, Thornagel (2009) demonstrated that local shear rate gradients force powder particles to leave areas of high gradients, thus making them the trigger for phase separation, Wall slip in highly filled suspensions is closely related to migration effects. It is a rheological phenomenon which might serve as an indicator for phase separation occurring during the processing of highly filled compounds, because it represents an often used practical approach to avoid powder binder separation.

The purpose of this thesis is to study the rheological behaviour of highly filled (60 % by volume) polymer melts, employed in powder injection moulding (PIM) with the special emphasis on the wall-slip phenomenon. The theoretical part describes specifics of rheological behaviour of highly filled polymer melts such as phase separation and the occurrence of wall-slip in different geometries, and also introduces PIM technology in general. The experimental part includes the study of continuous processing of PIM feedstocks with the use of online rheometry.

## **I. THEORETICAL PART**

# 1 Highly filled polymer materials

Suspensions which are filled with solid particles close to their maximum packing fraction are encountered in a number of industries. Such materials include food products, polymeric composites, ceramics, detergents and soaps, filled elastomers, coal and energetic compounds. Highly filled suspensions, regardless of the diversity of their applications, exhibit various common rheological and processing traits which have been a subject of numerous investigations. The research of the flow and deformation behaviour of concentrated suspensions has been generally restricted to solid concentrations, which are below sixty-four percent by volume (Kalyon, 1993). Highly filled polymer melts are considered to be suspensions, thus this term can be also used in the following.

In highly filled polymer melts the polymer matrix serves as a carrier for the solid particles. The requirement is to obtain as low viscosity as possible at high particle loadings (Drzal; Shull, 2004). The information about dependence of the shear viscosity on the filler content, particle size, particle size distribution, particle shape and orientation in the flow field is summarized in various extensive reviews, including those by Jeffrey and Acrivos (1976), Mewis and Spaul (1976), Onogi and Matsumoto (1981), Metzner (1985), Kamal and Mutel (1985), Khan and Prud'homme (1987) and Barnes (1989). The majority of these studies have utilized the Couette flow, which involves the migration of the solid particles and the resulting concentration gradients (Kalyon, 1993).

Highly filled polymer melts, even if in the case of a Newtonian polymer medium, show the properties of non-Newtonian liquids, namely a pseudoplasticity, dilatancy and thixotropy. A common problem in using polymer melts of finely dispersed solid phase as filler is the agglomeration and flocculation of particles. The increased surface activity of the disperse phase is connected with the ability of particles to form stable coagulative structures in polymeric media (Palcevskis et al., 2005).

## 1.1 Powder injection moulding

One of the innovative technologies used for fabricating highly filled polymer compounds is the powder injection moulding (PIM), which will be further described in more details. It is well established and promising technology suitable for the mass fabrication of relatively small and complex net shape products with high density made from metals, ceramics, cemented carbides and cermets. This technology represents a challenging production method for automotive, medical, IT, military and other items as is

an alternative to machining and investment casting when fabrication via classic route is inappropriate. Some hard materials such as steel, zirconia, titanium or tungsten alloys prove to be difficult and expensive to grind or machine, therefore products that require materials with poor machinability or have difficult geometries are good candidates for PIM (Johnson, German; 2003). PIM offers advantages in comparison to conventional metal cutting or metal forming processes as it is a no scrap technique suitable for designs difficult to machine (Hausnerova, 2011). Furthermore, PIM overcomes the dimensional and productivity limits of isostatic pressing and casting, the defects and tolerance limitations of investment casting, the mechanical strength of die-cast parts, and the shape limitation of traditional powder compacts (Gonzalez-Gutierrez et al., 2011). The process combines the shape making capability of plastic injection moulding with the material flexibility of powder metallurgy. A great potential of PIM technology is its ability to combine multiple parts into a single item and the possibility of integration of various effects without additional operations (Hausnerova, 2011).

Powder injection moulding is a combination of four sequential technological processes – feedstock preparation, injection moulding, debinding and sintering – all of which have an effect on the properties of the final parts. Fig. 1 schematically presents the whole process. The feedstock, which has to be as homogeneous as possible, is made by intensive mixing of the metal powder and the binder. A highly (typically around 60 vol. %) concentrated compound is then processed in injection moulding machines utilized in the plastics industry to obtain a green part. In this step the feedstock is formed into the desired shape. In the next phase, the binder is chemically or thermally removed from the moulded green part in various debinding processes. The brown part that is produced retains its shape

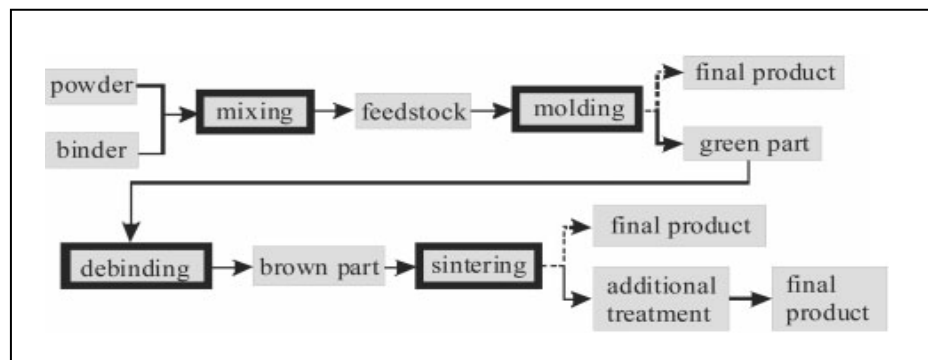
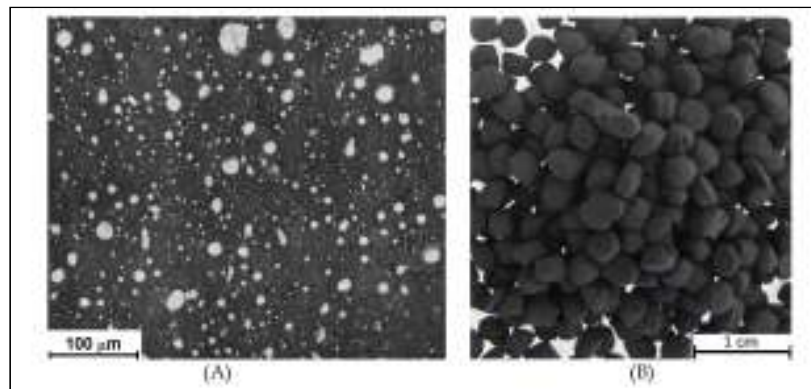


Fig. 1. Schematic representation of PIM (Berginc et al., 2007)

owing to the friction between the particles of metal powder. This part is very fragile and needs to be sintered carefully to achieve its final sintered density and the desired mechanical, chemical and dimensional properties. The final properties of the product can be further improved with additional heat and mechanical treatments (Berginc et al., 2007; Gonzalez-Gutierrez et al., 2011; Hausnerova, 2011).

### 1.1.1 PIM feedstock preparation

The first task to be considered when planning PIM production is to select material – powder and binder. The binder and powder are mixed above the melting point of the binder constituents to provide a uniform coating on the powder surface. This technique requires preparing a feedstock, in which individual powder particles are fully covered (lubricated) with the smallest effective amount of a binder (Fig. 2). Nevertheless, a current trend is to buy commercial, ready to use feedstocks in the shape of pellets based on a patented binder system mixed with different powders (Hausnerova, 2011).



*Fig. 2. (A) Micrograph of feedstock material showing metallic particles surrounded by polymeric binder, (B) Pellets of commercially available feedstock material Catamold® by BASF (Gonzalez-Gutierrez et al., 2011)*

A homogenous distribution of binder and powder particles in feedstock helps to minimize segregation during the injection moulding stage and later on to obtain isotropic shrinkage after debinding and sintering. The homogeneity of feedstock materials can be influenced by the technique used for mixing of individual components. Feedstocks can be either produced in a batch process (high-shear mixers, roll mills) or continuously (screw extruders, shear rolls). When using fine particles, which have a tendency to agglomerate, batch mixing in z-blade mixers is preferred, even though the process can take a couple of hours (Gonzalez-Gutierrez et al., 2011).

When selecting a material for a PIM component, both the economics and the final properties must be considered. The availability and cost of PIM quality powders are still major limiting factors affecting decision making. Powder cost impacts final component cost, but powder availability is the first consideration. Nevertheless, any metal (except for pure aluminium, due to an oxide film on the surface inhibiting sintering) or ceramic powder can be utilized in both PIM divisions (MIM – Metal Injection Moulding and CIM – Ceramic Injection Moulding) if it is prepared in the suitable form (German, 1990).

Important powder characteristics such as particle size, particle size distribution and shape of particles are influenced by the way of their preparation. Three starting possible forms of powders are mixed elemental powders, fully compounded powders or a hybrid of partially compounded and elemental powders (Johnson, German; 2003). The pre-alloyed powder often proves to be easier to process but it is more costly. A wide variety of materials is available in the needed small particle sizes. However, the bulk of the PIM products fall into only a few categories:

- ferrous alloys such as steels, stainless steels, tool steels, high speed steels, iron-nickel magnetic alloys, and ferrous alloys such as Invar and Kovar,
- common oxide ceramics, such as alumina, silica and zirconia, and their mixtures,
- tungsten alloys, including both tungsten heavy alloys and tungsten-copper,
- cermets (such as Fe-TiC), cemented carbides (WC-Co) and related hard materials.

Besides these common ceramics and alloys, activity is emerging in special materials, which included precious metals, titanium alloys, nickel-base superalloys, molybdenum-copper, and non-oxide ceramics such as silicon carbide and silicon nitride (Johnson, German; 2003).

The binder component gives to the mixture compound the flow characteristics of a highly thermoplastic fluid. It means that feedstocks can be processed in moulds with complex geometries as in standard polymer injection moulding. Perhaps the most widely used binder is the polyacetal (Catamold® BASF), which provides good processability and excellent shape retention. However, its removal is carried out in a highly concentrated nitric acid, and thus its utilization brings enhanced concerns for health and safety regulations. Such an issue can be overcome with water-soluble binders based on polyethylene oxide or polyvinyl alcohol, which are increasingly being employed (Hausnerova, 2011).

### 1.1.2 Injection moulding

Injection moulding is a technique during which the feedstock is formed into the desired shape and is performed at the temperature/pressure conditions prescribed for the selected feedstock. Although moulding of the PIM compounds is comparable to the injection moulding of plastics, the machines are usually optimized for the processing of powdery materials with a wear-resistant components (such as cylinders, screws, non-return valves and moulds), a screw geometry adapted to lower compression rate and extended compression zone compared to standard screws for thermoplastics (Hausnerova, 2011). Due to the size of moulded parts, compression ratios used in PIM tend to be in the lower range. Ratio of 1.6 is considered to be optimal for the removal of air between granules (Gonzalez-Gutierrez et al., 2011).

The most popular method of PIM injection moulding is to use a reciprocating screw, horizontal, hydraulic or electric machine in which a screw stirs the pelletized feedstock inside the barrel while it is melting. The heating system brings the material to an appropriate temperature for easy flow. The solid feedstock pellets cause the most abrasive wear in the feed section of the screw, thus the feedstock should be melted as early as possible in the injection cycle. After melting the feedstock the screw acts as a plunger to compress the material and remove any bubbles. The melted material is injected into the mould through the nozzle under high pressure (60 MPa or even more). After cooling and solidification of the binder, the nozzle is pulled away from the mould. Due to the fragile nature of most green parts, it is removed from the mould by robotic system in order to prevent the impacts which could deform or even break the moulded part (Gonzalez-Gutierrez et al., 2011).

Design limitations include uniform or gradual section thickness changes, minimized wall thickness (reducing not only material consumption and moulding cycle time but considerably also debinding and sintering), round corners to reduce stress concentrations and risk of fracture, and minimum undercuts on internal bores. Contrary to conventional injection moulding, for PIM it is important to design items with one flat surface which allows standard support trays during sintering, otherwise special trays are required (Hausnerova, 2011).

## 2 Rheology of highly filled systems

The interpretation of the rheological behaviour of highly filled (typically above 50% by volume) systems is definitely a difficult task. Honek et al. (2005) have shown that the predicting of the flow properties of such complicated filled suspensions brings many obstacles and limitations because of the multi-component character of binder and complex powder characteristics, mainly irregular shape and broad particle size distribution.

The reasons for the absence of new analysis describing the flow of the highly filled polymer materials are the theoretical and experimental difficulties encountered in investigating these systems such as sensitivity to the preparation, deformation history, very narrow (with respect to deformations) region of linearly viscoelastic reaction and possibility of slippage of the material along the working surfaces of a measuring device, which affects the repeatability of results. The reaction of highly filled systems to deformation is a complex combination of viscous, elastic, and plastic effects, which strongly depend on the conditions and history of sample deformation (Drzal; Shull, 2004).

### 2.1 Rheological approaches to optimize PIM process

The improving of the properties of every single component in PIM material has a great importance to the optimization of process. Rheology represents a powerful tool in the treatment of several quality determining factors of the PIM process. The behaviour of feedstocks during the injection moulding should follow that of the other shear thinning fluids. The increase in the shear rate causes the fluid's viscosity to decrease, which is then used (Berginc et al., 2007). Ahn et al. (2009) mentioned that a high drop in viscosity at high shear rates is a desired property for cavity filling with less energy, especially for complicated geometries (Gonzalez-Gutierrez et al., 2011).

#### 2.1.1 Binder formulation

The rheological properties of a binder are important to determine the optimal binder formulation or to select a proper additive. It is important to keep the viscosity of the binder as low as possible in order to facilitate the injection moulding process. However, low viscosity materials have also low mechanical properties when solidified. For this reason, a compromise between the flow properties and the solid mechanical properties of binder has to be made.



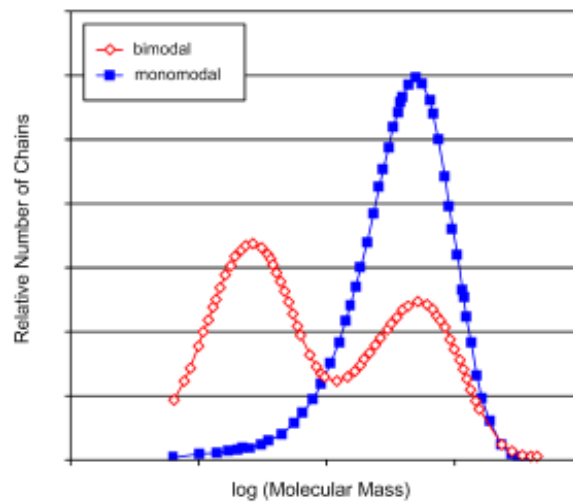


Fig. 3. Schematic representation of bimodal and monomodal molecular mass distribution in polymeric materials (Gonzalez-Gutierrez et al., 2011)

Recent investigations have shown that bimodality in the molecular mass distribution (Fig. 3) of binders has got a great potential to lower the viscosity of the feedstock in the molten state and maintain the mechanical strength of the green part without modifying the chemistry of the binder. The addition of small polymer chains increases the flowability of the binder in the molten state, since such small molecules can act as internal lubricants for the larger molecules facilitating their movement. However, when the binder is in a solid state the smaller molecules can fit between the larger ones, creating a closely packed structure that cannot be deformed easily, and thus improving the mechanical properties (Gonzalez-Gutierrez et al., 2011).

Once good flowability of the binder has been obtained, it is important to check the flowability of the feedstock material. It will not only depend on the viscosity of binder but also on the powder loading. A capillary rheometry is currently recognized as the best approach to predict the flow behaviour of PIM compounds. This approach, however, is complicated by several factors such as flow restrictions caused by instabilities or the so-called Serge-Silberberg effect, it is a movement of particles from the capillary wall to the centre during flow, which leads to an axial solids concentration gradient. In the case of binders, a capillary rheometry is difficult to realize due to low viscosity. Instead, rotational rheometers of cocylindrical geometry are preferred (Hausnerova, 2011).

The viscosity of ADVAMET 316L feedstock was measured (Berginc et al., 2007) with using a parallel plate rheometer and capillary rheometer. The conditions in the latter

method are similar to those during the real process of the injection moulding and extrusion, and thus this method is appropriate for viscosity measurements of polymer materials. The biggest disadvantages are pressure drop at the entrance to the capillary, melt heating, and the dependence of viscosity on pressure. For an exact determination of the viscosity for non-Newtonian fluids, the Weissenberg–Rabinowitsch and Bagly corrections are used.

### 2.1.2 Determination of powder/binder ratio

As already mentioned, the rheological properties of feedstock are not influenced only by the binder's viscosity but also by the powder loading. The optimum of powder loading within a feedstock refers to a powder concentration for which a compound exhibits good flow properties for the purpose of PIM (viscosity less than 1000 Pa.s), as well as homogeneity and stability in the shear rate range of  $10^2 - 10^5 \text{ s}^{-1}$  (Dihoru et al., 2000).

The powder content usually ranges from 50 to 65 % in volume, although there are some claims of optimized commercial formulations in which even more than 80 vol. % is used (German, 1990). If the powder content is found to be lower than 50 vol. %, the sintering ability of the feedstock and the final density of the part are significantly lowered (Gonzalez-Gutierrez et al., 2011). It was reported in experimental study (Dihoru et al., 2000) that the optimal solids loading of feedstocks consisting of blends should be set at 6-14 % lower than the critical value attainable for a given system.

There are generally three approaches to determine the maximum powder loading: density measurement, mixing torque evaluation, and rheological tests. When using a torque evaluation, the critical solid loading corresponds to the concentration of powder for which the measured torque becomes unstable and an increase in its value occurs (Dihoru et al., 2000). Nevertheless, rheological investigation of capillary flow data still represents the most sophisticated evaluation of optimum loading, using the relative viscosity (ratio of a feedstock viscosity to the viscosity of a binder) as a variable to obtain maximum packing fraction for a particular powder-binder compound. As a powder concentration reaches the maximum, all of the binder is confined among powder particles and the flow of the feedstock is restrained, resulting in a sharp increase in relative viscosity (Hausnerova, 2011).

A value of the maximum packaging of feedstocks is influenced by the properties of powder as well as packing procedure (German, 1990). The packing behaviour of particulate materials depends largely on their particle size, shape and surface characteristics. In order to increase the packing fraction of powders, small particles to fill in the pores in the packed

structure obtained from larger particles are used and then even smaller particles to fill in the remaining pores and so on. This approach is known as multimodal packing and much effort has been devoted to find the optimal particle size ratios that yield maximum packing fractions (Rothon, 2003).

According to German (1999) an ideal PIM component should combine large and small particles in a tailored particle size distribution. Further rheological measurements (Hausnerova et al., 1999) showed that feedstock material containing particles with a bimodal particle size distribution exhibits lower viscosity compared to feedstock with monomodal powder. It supports the findings of Chang and Powell (1994) and Metzner (1985), which verified that viscosity can be significantly reduced for powders with large differences in size by adding smaller particles, which fill the inter-particle voids, releasing previously immobilised fluid (Hausnerova, 2011).

A large particle size ratio can also provide higher packing density, better stability in debinding, good mouldability and lower shrinkage during sintering. Thus, by mixing a much cheaper large and irregular powder with powders typically used for PIM or with another irregular powder, blends with good packing and flow properties, and also the appropriate cost can be obtained (Dihoru, 2000). Spherical or rounded shaped small powders are preferred due to their easily predictable flow behaviour during mixing with a binder and injection moulding of feedstock, but the risk of poor shape retention is enhanced (Hausnerova, 2011).

According to German (1990) more than a hundred empirical and theoretical relations have been proposed in order to obtain the value of maximum packing fraction from the relative viscosity data. The capillary flow data of multi-component polymer binder-based on polyethylene, paraffin, ethylene-based copolymers, and polyethylene glycol-compounded with three various hard-metal carbide powders were employed (Honek et al., 2005) to test over 15 mathematical models proposed for highly filled systems. The first two powders had unimodal particle size distribution varying in the portion of small particles (below 1  $\mu\text{m}$ ), while the third powder had a bimodal one. The shape of the particles was irregular. It was found that the particular values of maximum loadings are in good accordance with the predictions based on powder characteristics. The highest value of maximum loading (0.69 derived from a linearized Mooney model) corresponded to the powder with the broadest distribution of particle sizes, while the lowest value (0.53 from the Frankel-Acrivos model) was attained for powder with a bigger aspect ratio of the particles.

### 2.1.3 A phase separation

Highly filled polymeric compounds naturally exhibit rather complex flow behaviour accompanied with separation of material components (powder and polymer) during high shear deformation processes. An understanding of rheology of such systems thus plays a crucial role in solving the critical quality issues of the process. In some cases, a portion of final parts that does not meet the quality requirements, may reach up to 25 % of the production (Williams, 2009).

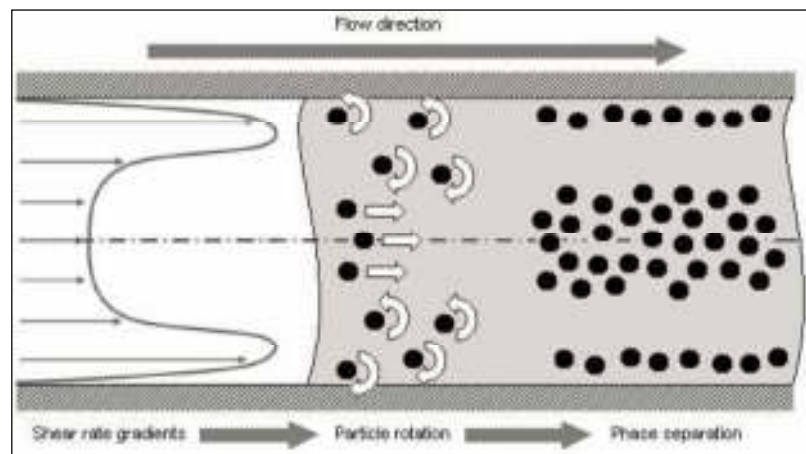


*Fig. 4. Flow pattern of highly filled polymer material across the channel causing powder - binder separation (Thornagel, 2009)*

Currently, the separation of polymer and filler components during mould filling is the main critical processability point. However, its mechanism is still not fully understood much like its onset and extent is not quantified. Thornagel (2009) has demonstrated (assuming no slip and good adhesion of feedstock to the channel wall) that the phase separation might arise as a consequence of local shear rate gradients occurring close to the wall of the flow channel (Fig. 4). Particles flowing in the peak area close to the wall show non-uniform shear rates leading to their rotation, which increases in severity as the shear stress gradients grow. Rotating particles naturally move away from areas of high shear gradients to the middle of the flow domain, which is characterized by a plateau at a considerably lower shear rate level. As a result, high polymer content is typical for the area of the highest shear rate (Fig. 5), while the plateau of the lower shear rate accommodates powder rich material. The description of separation phenomenon is complicated by the fact that the separation pattern changes continuously. To predict such situation would require a multi-phase

simulation, taking into account individual compound components (Hausnerova, 2011; Hausnerova et al., 2011).

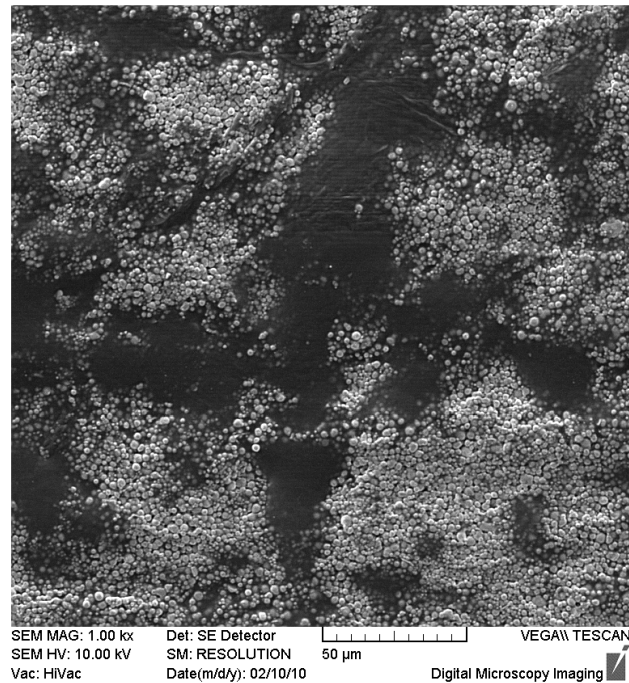


*Fig. 5. Detail of separated powder-binder area (Hausnerova, 2011)*

Prediction of a separation onset and its development during the filling of the mould requires consideration of relevant processing factors and their relation to the separation phenomenon. It is necessary to use proper mould geometry. The testing moulds with spiral, square spiral and zig-zag design only partly fulfil the purpose of forcing phase separation during mould filling. Thus, a new design of the testing mould (Fig. 6) including inner and outer corners, radical thickness changes, weld lines and very thin film parts has been developed at the Polymer Centre TBU in Zlin in cooperation with IFAM, Bremen in order to investigate the phase separation phenomenon occurring at high shear deformations of highly filled polymer/powder compounds during mould filling (Hausnerova et al., 2011).

The important task in description of the phase separation is to propose the method of quantitative determination of separation severity. Differential scanning calorimetry (DSC) was employed (Jenni et al., 2008) to quantify local powder content, comparing the influence of injection moulding parameters on separation appearance with a software simulation based on the balance model of the flow of rigid, spherical particles in a Newtonian fluid. However, DSC has not proved to be a suitable approach to detect the changes in powder concentrations for compounds containing multiple polymer

components. Hausnerova et al. (2011) used scanning electron microscopy (SEM) combined with energy dispersive X-ray (EDX) analysis of the distribution of elements typical for powder and polymer to provide a quantitative evaluation of the powder-binder separation.

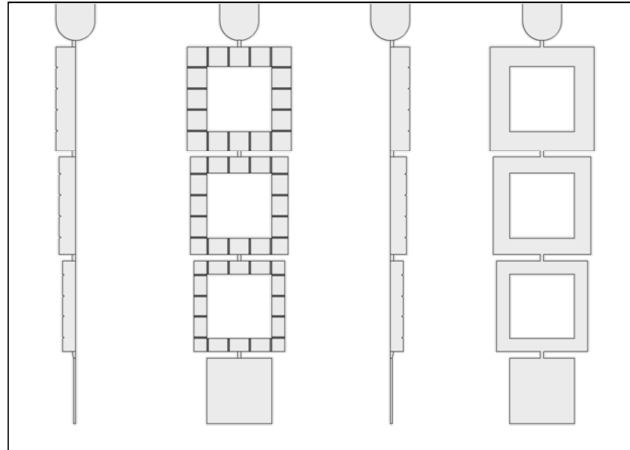


*Fig. 6. New design of a testing mould (Hausnerova et al., 2011)*

### 3 Wall depletion effect

Apparent wall slip (Yoshimura, Prud'homme, 1988; Barnes, 1995), yield stress (Isayev, 1987; Poslinski et al., 1988), pressure oscillations ( Yilmazer et al., 1989; Kalyon, Yilmazer, 1990; Isayev, Fan, 1994; Yaras et al., 1994) and other flow phenomena are present during the flow of two-phase (or multi-phase) systems such as suspensions of large or flocculated particles, emulsions of large droplet size or pastes. In these cases, large means multi-micron. Many empirical measurements have proved that wall-slip depletion serves as an indicator of non-separation such systems. Wall effects have been known since flow curves were plotted properly. A work performed by Bingham and his school before 1930 showed a slip layer at tube walls. Bingham (1922) stated that it is quite possible that the fluidity of a liquid near the surface is not identical with that within the body of the liquid. Before that Reiner quoted Green in 1920, who understood that a liquid layer of the dispersion medium of a suspension is formed near the walls of flow tubes, and acted as a lubricant (Barnes, 1995).

As Barnes stated, the wall slip more precisely occurs in the flow of such mentioned systems because of the displacement of the disperse phases away from solid boundaries. This phenomenon leaves a low viscosity depleted layer of liquid at a wall. The simplest picture we could imagine as the end result of slip is a very thin continuous-phase-only-layer left at the boundary, and the bulk flow with original concentration. The creation of such a thin layer with lower viscosity than a bulk flow causes that any liquid slips along the wall because of the lubrication effect. As a concentration of the system increases, the layer becomes thinner and thinner because it is more difficult to create with the large reverse osmotic force present. However, the enormous increase in the bulk viscosity with increase in concentration means that although thinner, the layer becomes, paradoxically, even more important. It is possible that very viscous liquids such as polymer melts do lose complete adhesion with respect to the walls and slide along them, sometimes intermittently in a stick-slip way (Barnes, 1995).

Many concentrated suspensions slip due to the formation of a binder rich region next to the wall. However, elastomers are susceptible to slip even without lubricating fluid layers, sliding at the tool interface if there is insufficient friction (Nickerson, 2005). The occurrence of wall slip decreases the deformation rate imposed on the suspension in comparison to the no-slip condition under similar wall shear stress (Kalyon, 1993). In measurements of fluid's viscosity it is necessary to correct for wall slip to determine the

true deformation experienced by the bulk of the sample and the true viscosity (Yoshimura, Prud'homme, 1988).

### 3.1 Phenomena that give rise to wall depletion

When a two-, or more, phase liquid is brought into contact with a smooth, solid boundary, the local microstructure is first affected by physical depletion because the suspended particles cannot penetrate solid walls. This phenomenon called the static (no-flow) geometric depletion effect is present even without flow and automatically leads to a shear-rate gradient near the wall, which will then enhance the dynamic depletion.

Sometimes the walls themselves can repel adjacent particles because of various physico-chemical forces arising between the particles and the walls, e.g. electrostatic and steric. When flow takes place in the bulk fluid, the resulting hydrodynamic and entropic forces can move particles away from walls. Deformable particles will always move away from solid boundaries, even when no shear-rate gradient exists in the equivalent single-phase flow (e.g. small-angle cone and plate, narrow-gap concentric cylinders), but solid particles only move normal to walls when there is a shear-rate gradient away from the wall, as for instance in tubes. A number of forces are present to oppose this movement of particles away from the wall into the bulk, the most important is osmotic pressure arising from the concentration gradient created (Barnes, 1995).

The following conditions usually lead to large and significant slip effects:

- large particles as the disperse phase,
- a large dependence of viscosity on the concentration of the dispersed phase, smooth walls and small geometry size,
- usually low flow rates (effect is greatest at low speeds, although centripetal artifactual effects can be seen at high speeds of rotation)
- walls and particles carrying like electrostatic charges and electrically conductive continuous phase.

### 3.2 A manifestations of slip

In many cases the slip effects seen in viscometers need to be characterised because they can also be seen in flow in smooth pipes and conduits during the manufacturing processes such as screw extrusion. This is usually done by relating the wall



shear stress to a slip velocity using a power-law relationship. When the bulk flow has already been described, the flow in real situations can be calculated.

The most obvious manifestation of slip is based on comparing viscosities obtained from different size geometries with calculated viscosity from formulae that assumes no slip in the flowing liquid. In particular the apparent viscosity calculated in this way always decreases and the apparent wall shear rate increases with decrease in geometry size (tube radius, gap size, cone angle) at the constant wall shear stress as shown in Fig. 7, which in other words means that slipping is more significant (Barnes, 1995). In each set of data the apparent viscosity values obtained employing various dies that have different diameters do not overlap.

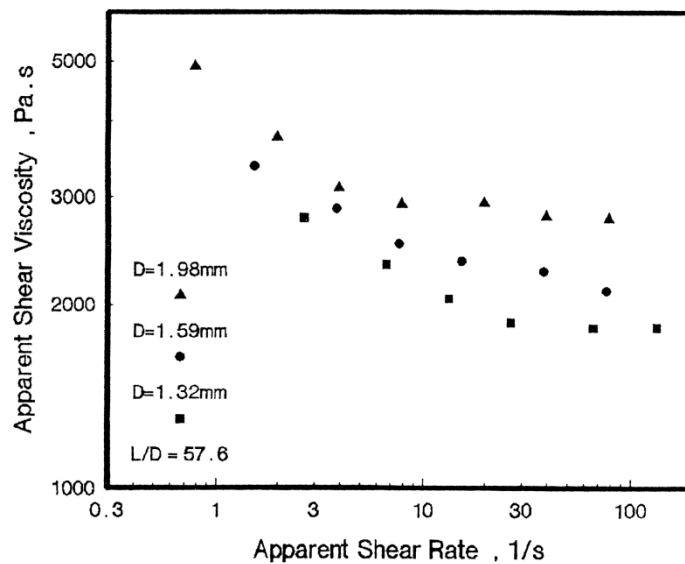


Fig. 7. Apparent viscosity versus shear rate obtained with capillaries of  $L/D$  ratio of 57.6 (Kalyon, Yilmazer, 1990)

To characterize the wall slip behaviour and to correct the rheological characterization data collected for wall slip, Mooney (1931) proposed a method for evaluation of data from capillary and Couette flow to determine the slip velocity from the slope of the apparent shear rate versus reciprocal diameter or gap data collected at constant wall shear stress. His solution was based on measurements with three capillaries with different diameter but constant  $L/D$  ratio, and three different gaps for concentric cylinders, respectively (Kalyon, 1993). Mooney's analysis states that in capillary flows the apparent shear rate at the wall,  $\dot{\gamma}_a = 8V/D$ , is given by Eq. (1):

$$\frac{8V}{D} = \frac{4}{\tau_w^3} \int_0^{\tau_w} \tau^2 \dot{\gamma} d\dot{\gamma} + \frac{8u_s}{D} \tag{1}$$

where  $V$  is the average velocity of the fluid in the capillary,  $D$  is the capillary diameter,  $\tau$  is the shear stress,  $\tau_w$  is the shear stress at the wall,  $\dot{\gamma}$  is true shear rate and  $u_s$  is the slip velocity at the wall (Kalyon, Yilmazer, 1990). Upon differentiating the both sides of the equation with respect to  $1/D$  at constant  $\tau_w$  and rearranging, the slip velocity is obtained from the Eq. (2):

$$\left| \frac{\delta (8V/D)}{\delta (1/D)} \right|_{\tau_w} = 8u_s \tag{2}$$

The slope of the straight line obtained from the plots of the apparent shear rate versus reciprocal of capillary diameter  $1/D$  equal to  $8u_s$ . The analysis is illustrated in Fig. 8 for a highly filled suspension consisting of 76.5 % volume solids with a bimodal particle size distribution.

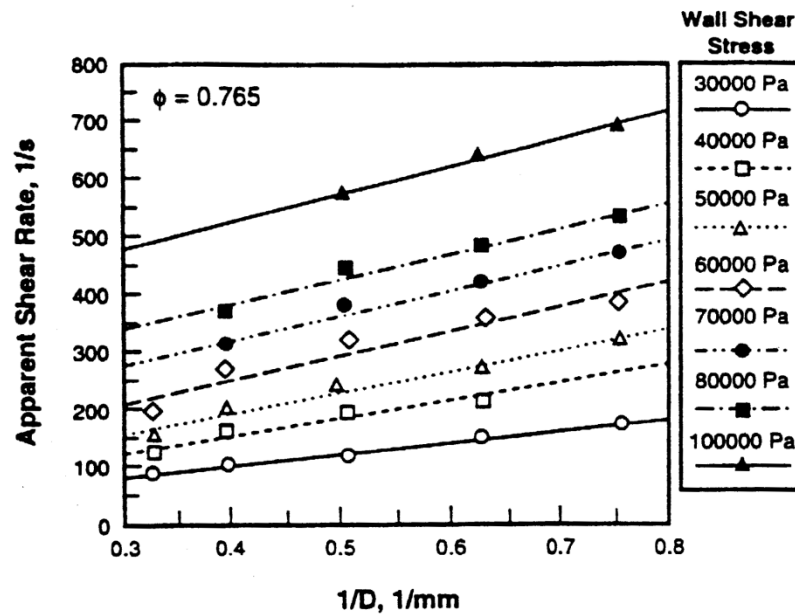


Fig. 8. Apparent shear rate versus reciprocal of capillary diameter,  $1/D$ , for a suspension consisting of 76.5 % by volume solids in capillary flow (Kalyon, 1993)

Incorporation of Jastrzebski interface condition has become widely accepted in cases where classic Mooney’s approach gives unviable results. Nevertheless, Martin and Wilson (2005) recommended more recently usage of Tikhonov regularization method of Mooney’s analysis for capillary data treatment.

The presence of slip can be also detected from single geometry measurements. Some other effects can be expected in a flow curve such as unexpected lower Newtonian plateaus,

sometimes with a pseudo-yield stress at even lower stresses, as well as sudden breaks in the flow curve at higher shear stresses/rates (Barnes, 1995).

A typical flow curve with wall slip measured over a wide enough range of shear stress is shown in Fig. 9. The smooth geometries give an early and faster-than-expected drop in viscosity. This often precipitous drop usually occurs at a shear stress or shear rate below that of the normal decrease in viscosity due to microstructural changes and static depletion. Below this drop, the viscosity curve often levels out onto a pseudo-Newtonian plateau, which stretches out nearly to the normal flow curve and appears to rejoin it, although possibly just below it. Where the pseudo-plateau rejoins the flow curve, the change in curvature can be quite sharp. Some workers have studied and stated this plateau and turn-ups at lower shear rates as a yield stress (Barnes, 1995).

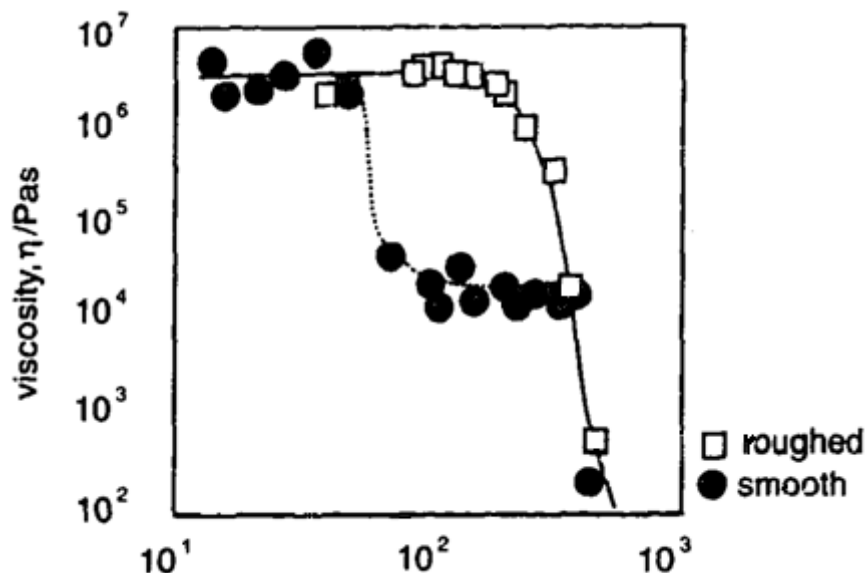


Fig. 9. Viscosity vs. shear stress for a printing ink, measured in a parallel-plate geometry with smooth and roughened plates (Barnes, 1995)

The flow curve can also be replotted as wall shear stress against shear rate. Equally, if the flow curve is plotted as viscosity against shear rate, the effects that are pointing to the wall slip often go unnoticed.

### 3.3 Approaches to eliminating of slip

Wall slip is a constant concern for rheologists working in fields ranging from biomaterials and gels to industrial and food products and personal-care items. A number of

useful solutions to the wall-slip problem in its various forms have evolved for specific cases (Nickerson, 2005). By contrast, in many cases wall slip is a desirable effect and need to be characterized, not eliminated, as in the case of this thesis when it is considered as a qualitative parameter indicating powder-binder separation absence/occurrence during the processing of PIM materials. However, sometimes when trying to understand the microstructure/flow interaction in the bulk of the material, the wall slip has to be eliminated (Barnes, 1995). These wall-slip prevention methods have been divided into three general approaches: mathematical methods, surface modifications, and alternative geometries. Each method has made important contributions to the field, but each has significant limitations as explained below (Nickerson, 2005).

The first approach involves empirically or mathematically determining of magnitude of the wall slip and accounting for its contribution to rheological measurements, as explained by Yoshimura and Prud'homme (1988) and Barnes (1995). Mathematical methods can be very useful, because they include the solutions when the wall slip is characterized rather than simply eliminated. However, mathematical methods require repetitive experiments and large sample volumes, which can be prohibitive (Nickerson, 2005).

Slip effects in viscometers or rheometers can usually be coped with if they are confined to very thin layers, and no gross changes occur in the bulk of the fluid. Then the overall flow can be split into the slip flow operating at the wall, and the bulk flow flowing normally within it with an added boundary velocity. Afterwards, by giving enough data - including a number of geometry sizes, the flow can be resolved into the separate components, each mathematically describable. However, the concentration gradients can range over such length scales in the case of concentrated suspensions of large particles, thus it is simply impossible to think that one is rheologically characterising a given system (Barnes, 1995).

Another approach is to prevent slip by modifying the surfaces of standard rheological tools. To eliminate the effect of the slip, the nature of the walls has to be altered. This is usually accomplished physically by either roughening the surfaces or profiling. Sandblasting or attaching rough or profiled material to plates has also been used. Buscall et al. (1993) may be a good example of the use of profiling by sandblasting, and Gregory and Mayers (1993) by bonding a rough surface to their parallel plates, for example sandpaper (Barnes, 1995). In some cases the chemical modifications of the wall can be used to eliminate repulsion effects by the absorption of certain chemical species in order for instance to change the nature of the electrostatic charge on the wall (Barnes, 1995).

Surface methods have been successfully applied to systems that form thin slip layers. Unfortunately, this method is not always useful and slip can still persist with surface modified tools in many systems, particularly gels and elastomers. Also, to be effective in gels and solids, most surface-modified tools require compression or significant normal force as described by Jin and Grodzinsky (2001) and Liu and Bilston (2000). Typical samples are compressed a minimum of 5 – 10 %, which can alter the structure of the material (Nickerson, 2005).

The third approach to the wall-slip problem is to use alternative geometries such as the vane by (Barnes, Nguyen, 2001) and helical (Cullen et al., 2003) tools, which either prevent the formation of slip layers through mixing or measure the properties of the sample in spite of the slip layer. The usage of popular vane geometry has the advantage because it is easy to make and clean. The vane method has been successfully used by a number of groups to overcome slip, for instance the work of Meeten and Sherwood (1992) following that of Dzuy and Boger (1983) (Barnes, 1995). The disadvantage of using the alternative geometries is that most of them, particularly vane and helical tools, are also unsuitable for delicate samples which can be destroyed by loading into a highly non-uniform gap (Nickerson, 2005).

### **3.4 Slip in particular geometries**

Slip effects can potentially be present in all viscometers and rheometers because of the necessary presence of walls, but the effect is mostly seen in situations where, within the flow geometry, there is a shear-stress and shear-rate gradient away from the wall. A wall-slip effect can occur in several different geometries such as tubes, concentric cylinders, cone-and-plate or parallel-plate disks, or some novel tested geometries.

#### **3.4.1 Tubes**

Assuming that the wall-slip effect is simplified to the continuous-phase-layer with constant thickness and composition, the necessary theory for slip flow in a tube was worked out. It was shown, as mentioned above, that by plotting the apparent shear rate against the inverse of the tube diameter, an estimate of the slip flow and the bulk flow can be obtained. The assumption usually made for slip in tubes is that the shear stress is the same on both sides of the boundaries of supposed slip layer. This is reasonable because

such a layer is never more than a few microns thick, compared with a minimum of 1 mm tube diameter.

In tubes, there is a linear shear-stress gradient from the wall to the centre where the stress is zero. Therefore, the velocity of the slip layer is zero at the wall increasing towards to the centre of the capillary as shown schematically in Fig. 10, where  $D$  indicates diameter of the capillary and  $\delta$  is thickness of the slip layer (Barnes, 1995).

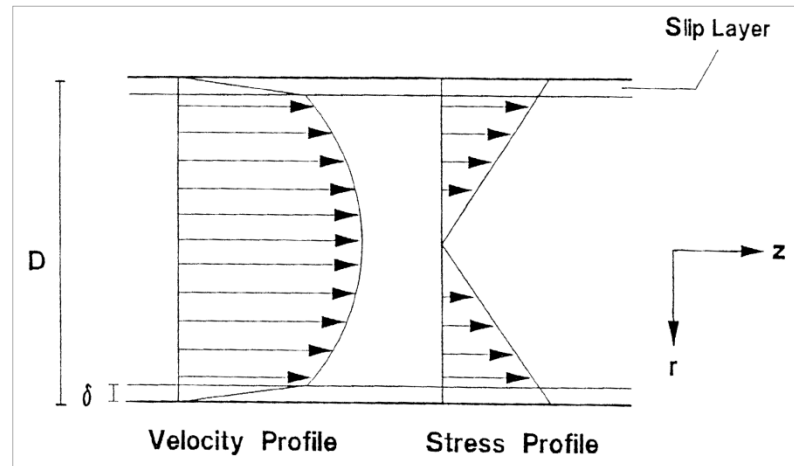


Fig. 10. Schematic representation of shear stress and velocity profile in capillary flow with apparent wall slip (Kalyon, Yilmazer, 1990)

Considering a plug flow, where the slip dominates the flow, there appears to be no velocity gradient in the inner core. As the shear stress is increased, the point comes where the shear stress is enough to produce a noticeable shear rate within the core material, because the viscosity has dropped considerably. If going to higher and higher shear stress, this shearing of the inner core results in a progressively more important contribution to the flow rate. Eventually, this effect becomes dominant, and the slip effect, although still present, becomes negligible in terms of its contribution to the overall flow rate (Barnes, 1995).

When describing the flow in a tube the effect of slip on the relative importance of the inlet flow should be also noted. If a material flowing into a tube from a larger container slips down the tube, the pressure gradient is much lower than would be found without slip. However, the pressure drop at the inlet will be little changed by the presence of slip, because it is dominated by the essentially extensional flow in the bulk of the fluid being deformed to enter the tube. Thus, the relative importance of the entry pressure with respect to the total pressure drop down the tube increases greatly when slip is present. It could in fact be the dominant effect for short tubes (nozzles) and easily be mistaken for a very large

extensional viscosity effect, so it has to be taken account of in attempting to model such flows (Barnes, 1995).

### 3.4.2 Cylinders

After slip in tube flow, concentric cylinders were the next geometry to be considered. Let's consider the situation described by Fig. 11, where the material is situated in wide-gap concentric cylinder viscosimeter, and flows not only under the application of stress, but also slips relative to the cylinders.

So long as the material slips on the outside cylinder, there is a shear-rate gradient away from the outer wall and shear rate decreases towards the inner wall, where there is a considerable wall-slip effect. If slip layer exists near the inside wall of concentric cylinder viscosimeter, the shear-rate gradient on the wall is adverse, and the shear rate increases away from the outer wall towards the inner cylinder. Thus we expect less slip on the outer cylinder. Buscall et al. (1993) have found this to be true for flocculated suspensions. Some observations have been carried out in which it was proved that while slip occurred on the inner cylinder, no slip was seen on the outer cylinder.

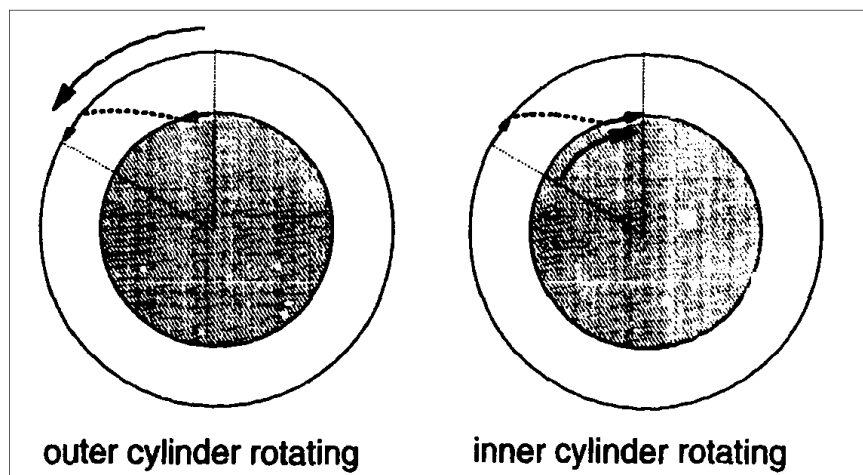


*Fig. 11. Representation of the flow field found in a wide-gap concentric cylinder geometry with slip at both the inner and outer walls, for either the outer or inner rotating (Barnes, 1995)*

It must also be remembered that for concentric cylinders any outwardly directed force as well as depleting the inner cylinder will tend to press the dispersed phase harder against the outside cylinder, which to some extent will overcome the depletion effect there. This is

why eliminating the slip at the inner cylinder alone by roughening, profiling, etc. is often enough to remove the slip effects in the complete geometry (Barnes, 1995).

### 3.4.3 Parallel plates

Accurate rheological characterization using rheometric flows depends critically upon the no-slip boundary condition, which essentially requires that the sample adhere to the surfaces of the rheometers. Specifically, the velocity of the sample at the sample boundary must be equal to the velocity of the adjacent tool surface (Fig. 12) so that the deformation rate

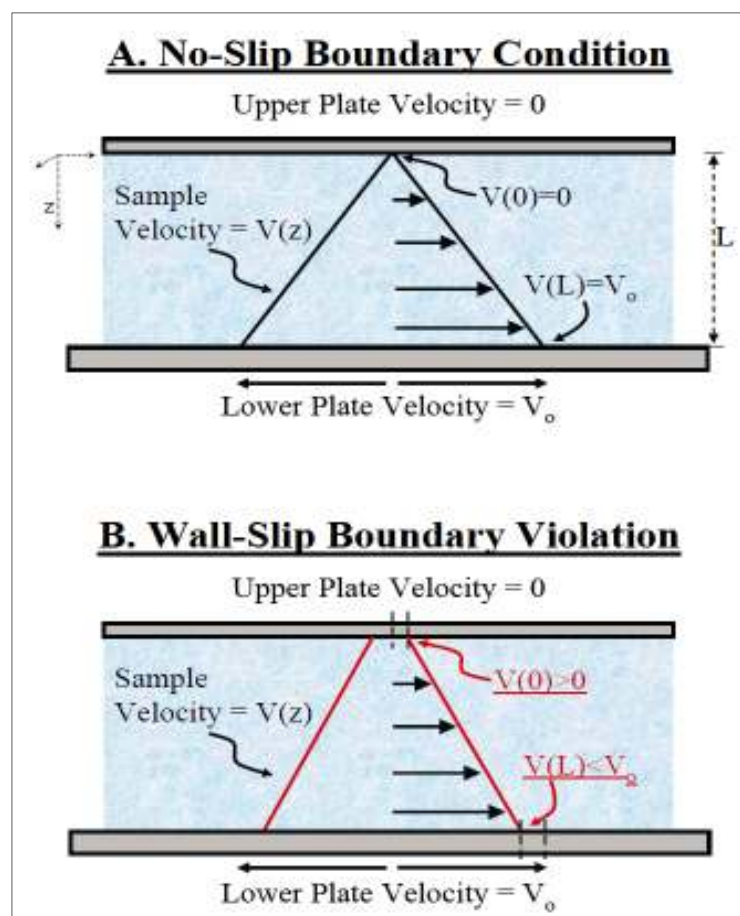


Fig. 12. Schematic representation of the velocity field in a sample experiencing shear deformation between parallel plates (A) when the no-slip boundary condition holds and (B) when it is violated (Nickerson, 2005)

of the sample is known. When a thin depletion layer forms, this boundary condition are violated, as for example in suspensions and emulsions. The depletion layer forms a planar region with reduced viscosity and so the deformation becomes inhomogeneous (Nickerson,



2005). The parallel-plate geometry has several experimental advantages for measuring fluid viscosities in the presence of wall slip.

In a smooth cone-and-plate or parallel-plate geometry compared with that in a smooth concentric cylinder viscometer, the slip effect can be enhanced by gravity for liquid systems that show any tendency to sediment or cream with time. In the horizontally aligned systems a continuous-phase-only-layer forms against the top or bottom plate respectively, not just a decreased concentration as in normal depletion. They will always slip irrespective of the value of the shear rate, especially if long-term experiments are performed. It could be suggested that gravity tends to push the particles against the wall. Though cone-and-plate and parallel-plate geometries are inherently more vulnerable to slip, because dispersions that have the kind of microstructure that gives slip often separate anyway under the action of gravity, for example large particles or drops, or flocculated suspensions. For the same liquid in a vertically aligned concentric-cylinder geometry gravity has no such effect and the normal depletion effects occur (Barnes, 1995).

Nickerson and Kornfield (2005) showed that novel cleat test geometry is a unique tool for slip prevention, which accommodates small sample volumes and overcomes many of the limitations occurring during the measurements in other geometries. The cleat geometry is a modified parallel-plate tool with a large number of uniform protrusions, or cleats of constant length ( $L_c$ , distance from plate face to cleat tip), extending from the faces of the plates. Densely packed protrusions penetrate the slip layer, preventing significant flow between cleats and their tips create a well-defined plane within the sample that is parallel to the plate face. There is a no-slip boundary below the tips, and the motion of fluid between the cleats decays to zero a short distance ( $\delta$ ) into the tool. The penetration depth  $\delta$  can be estimated from the geometric parameters of the cleats and verified empirically. The difference between cleat geometry and smooth plate experiments is the use of the effective sample gap ( $gap_{eff} = gap_{meas} + 2\delta$ ) instead of the measured sample gap. The effective sample gap boundary is established by the depth at which fluid motion is stopped. The position of this effective sample boundary was found to be independent of the material over the wide range of materials examined.

The cleat geometry suppresses slip without application of significant normal force as it is often required in surface-modified tools. The advantage of cleated tools over other slip-prevention methods is demonstrated using increasingly challenging materials – an emulsion (mayonnaise), a suspension (peanut butter), and a biological tissue (porcine

vitreous humor), that is difficult or impossible to handle successfully with prior tools (Nickerson, Kornfield, 2005).

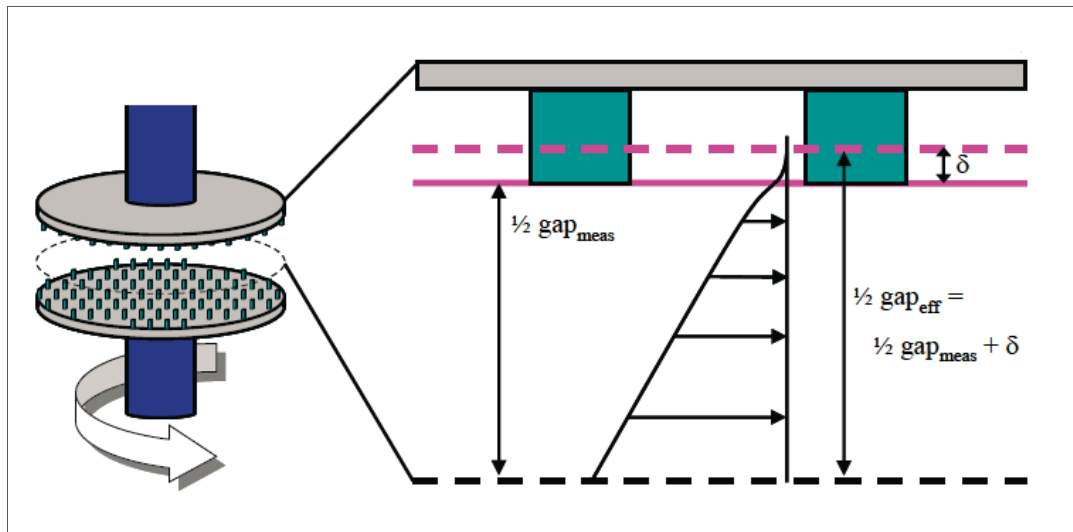


Fig. 13. Schematic representation of two cleated fixtures placed opposite each other. Sample motion penetrates only a short distance  $\delta$  into the cleat array (Nickerson, 2005)

## **II. EXPERIMENTAL PART**

## 4 Characteristics of feedstocks

Four types of commercially available highly filled materials were selected for the experimental measurements and analyses. The following feedstocks in the form of ready-to-mold granules were used to prepare studied samples:

- PolyMIM 17-4PH produced by polyMIM GmbH previously Polymer-Chemie GmbH
- PolyMIM 316L made by polyMIM GmbH produced by polyMIM GmbH
- Catamold 316L produced by BASF AG
- Embemold 17-4PH produced by BASF AG

The compared materials varied either in the type of used polymer-binder or powder composition. Although the composition of polymer matrix was unavailable by the manufacturers, the several conditions of injection moulding process and debinding process indicate the different material composition. The material characteristics of feedstocks are shown in Tables 1, 2, 3 and 4.

Table 1 Material characteristic of PolyMIM 17-4PH

PolyMIM 17-4PH							
<b>Material composition (as sintered; in weight - %)</b>							
Fe	C	Ni	Cr	Mn	Si	Cu	other
balance	< 0.07	3.0 - 5.0	15.0 - 17.5	< 1.0	< 1.0	3.0 - 5.0	< 0.45
<b>Typical properties</b>							
Sintered density $\geq 7.65$ g/cm <sup>3</sup>							
<b>Injection moulding process</b>							
moulding			Zone 1	Zone 2	Zone 3	Zone 4	Zone 5
45-65 °C			170 °C	175°C	180°C	185°C	190°C
<b>Debinding process</b>							
Solvent - water or distilled water							
Debinding temperature = 40 - 60°C							
Weight loss > 3.7 weight - %							
<b>Sintering process</b>							
Sintering atmosphere - 100% pure hydrogen							
Sintering temperature = 1350°C							

Table 2 Material characteristic of PolyMIM 316L

PolyMIM 316L							
<b>Material composition (as sintered; in weight%)</b>							
Fe	C	Ni	Cr	Mo	Mn	Si	other
balance	< 0.03	10.0 - 14.0	16.0 - 18.5	2.0 - 3.0	< 2.0	< 1.0	-
<b>Typical properties</b>							
Sintered density $\geq 7.75$ g/cm <sup>3</sup>							
<b>Injection moulding process</b>							
moulding			Zone 1	Zone 2	Zone 3	Zone 4	Zone 5
40-60 °C			180 °C	185°C	190°C	195°C	195°C
<b>Debinding process</b>							
Solvent - water or distilled water							
Debinding temperature = 40 - 60°C							
Weight loss > 3.6 weight %							
<b>Sintering process</b>							
Sintering atmosphere - 100% pure hydrogen							
Sintering temperature = 1360°C							

Table 3 Material characteristic of Catamold 316L

Catamold 316L G							
<b>Material composition (as sintered; in weight%)</b>							
Fe	C	Ni	Cr	Mo	Mn	Si	other
balance	$\leq 0.03$	10.0 - 14.0	16.0 - 18.0	2.0 - 3.0	$\leq 2.0$	$\leq 1.0$	-
<b>Typical properties</b>							
Sintered density $\geq 7.96$ g/cm <sup>3</sup>							
<b>Injection moulding process</b>							
moulding			Zone 1	Zone 2	Zone 3	Zone 4	Zone 5
128°C			160°C	170°C	180°C	190°C	190°C
<b>Debinding process</b>							
Solvent - HNO <sub>3</sub> > 98 %							
Debinding temperature = 110°C							
Weight loss > 7.6 weight %							
<b>Sintering process</b>							
Sintering atmosphere - 100% pure hydrogen							
Sintering temperature = 1380°C							

Table 4 Material characteristic of Embemold 17-4PH

Embemold 17-4PH							
<b>Material composition (as sintered; in weight%)</b>							
Fe	C	Ni	Cr	Mn	Si	Cu	other
balance	< 0.07	3.0 - 5.0	15.0 - 17.5	< 1.0	< 1.0	3.0 - 5.0	< 0.45
<b>Typical properties</b>							
Sintered density $\geq 7.96$ g/cm <sup>3</sup>							
<b>Injection moulding process</b>							
moulding			Zone 1	Zone 2	Zone 3	Zone 4	Zone 5
50-55°C			100°C	110°C	120°C	130°C	150°C
<b>Debinding process</b>							
Solvent – acetone							
Debinding temperature = 55°C							
Weight loss > 7.6 weight %							
<b>Sintering process</b>							
Sintering atmosphere - 100% pure hydrogen							
Sintering temperature = 1380°C							

## 5 Testing methods

### 5.1 Channel surface measurements

#### 5.1.1 Surface roughness

The measurements of surface quality of used flow channels were carried out on the machine Mitutoyo SJ-301, which is intended for contact measurements in a workshop environment. Measured values were determined from the vertical movement of the tip passing through the surface irregularities. The results can be displayed either graphically or numerically.

### 5.2 Rheological measurements

#### 5.2.1 Online rheometry

A slit die rheometry using speeds typical for extrusion process was set as a method suitable for the investigation of wall-slippage of PIM materials. The rheological measurements focused on wall-slip phenomena were performed on online rheometer (Brabender Extrusiograph 19/25D), usually used for testing the processability of thermoplastics. The material was first melted under defined conditions and then extruded through the slit dies (designed at TBU in Zlin) with dimensions either (10x0.5x100) mm or (15x1x100) mm. In order to study the impact of pressure conditions on wall-slip effect of the materials the dies were modified by insertion of movable solid valve enhancing the pressure growth on polymer melt. The valve was alternated in three positions; fully open, half-closed and fully closed. While the complete closure of the valve caused the greatest pressure growth on the polymer melt, in open position the pressure conditions were not enhanced at all. Moreover, the dies were equipped with five pressure transducers ( $p_1 - p_5$ ) in order to evaluate shear viscosity from pressure profile inside the die. Transducer  $p_5$  corresponds to pressure at the entrance to the flow channel ( $p_{entrance}$ ) and  $p_3$  to pressure at the exit of the channel ( $p_{exit}$ ). The sixth pressure transducer  $p_6$  was installed as control sensor whose value (700 bar) could not be exceeded. The scheme of arrangement of pressure transducers is shown in Fig. 14. The temperatures of individual zones (1 – 5) were controlled and displayed by electronic temperature controllers. All measuring values such as torque or pressure were recorded continuously and represented in the form of tables and diagrams parallel to the current test.

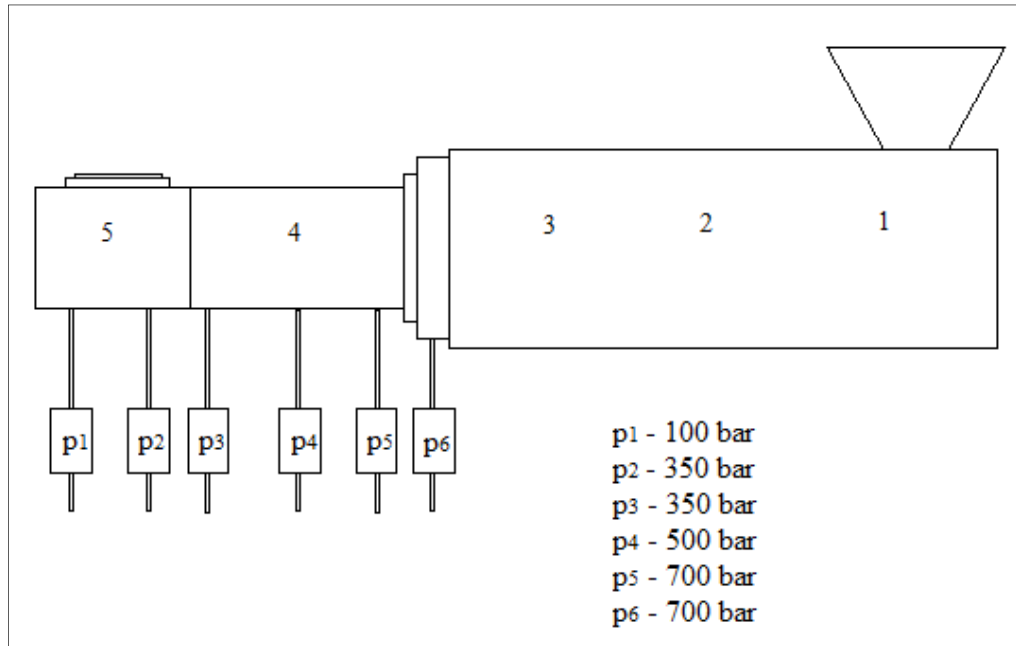


Fig. 14. Scheme of measuring device with representation of pressure ( $p_1 - p_6$ ) and temperature transducers ( $T_1, T_2$ ) and individual temperature zones (1, 2, 3 – extruder; 4 – slit die; 5 – movable valve)

### 5.3 Morphology measurements

#### 5.3.1 Scanning electron microscopy (SEM)

Scanning electron microscope from Tescan VEGA II LMU was used to investigate the particle shape and particle size distribution of the powder in the samples obtained at different shear rates. The instrument worked at 5 kV and the samples were coated with a thin layer of gold by using a polaron sputtering apparatus.

#### 5.3.2 Surface analysis

The surface roughness of selected samples was analyzed with the use of Talysurf CLI 500 system, which is essential tool for measurements of small surface components with its measuring envelope of (50x50x50) mm.



## 6 Results and discussion

### 6.1 Materials

Materials used for experimental measurements contain either the stainless steel powder with the 17-4 PH composition (polyMIM 17-4PH, Embemold 17-4PH) from which the majority of PIM automotive items are produced or stainless steel powder with the 316L composition (polyMIM 316L, Catamold 316L). The 17-4PH powder consists of approximately 17 % Cr, 4 % Ni, 4 % Cu, and low concentrations of alloying additions of manganese, silicon, niobium and tantalum. Good mechanical properties are probably the main reason of wide use of this composition. It gives fatigue strength over 500 MPa (Johnson, German; 2003), which is comparable to most wrought alloys. The stainless steel with the 316L composition consisting of approximately 17 % Cr, 12 % Ni and 2 % Mo is preferred mainly for medical appliances because of its combined strength and corrosion resistance. It shows an almost threefold increase in tensile strength and only modest decay in ductility at -253 °C compared with room temperature properties (Anonym, 2007), proved to be an excellent candidate for the BMW Hydrogen 7 car. A map of relative strength and relative corrosion resistance of 17-4PH and 316L powders in comparison with some other alloy grades published by Johnson and German (2003) is shown in Fig. 15. Although the higher-strength stainless steel grades are not as corrosion-resistant, the overall PIM process is competitive with other fabrication techniques.

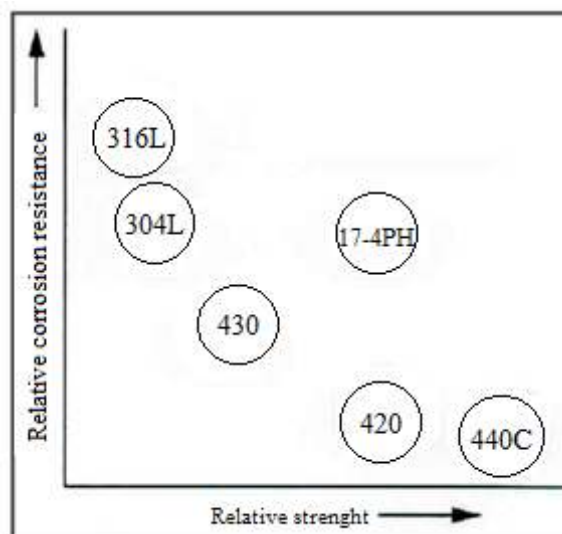


Fig. 15. Corrosion and strength attributes of the common PIM stainless steels (according to Johnson, German; 2003)

## 6.2 Geometry selection

Several present investigations are related to the development of devices for the measurement of rheological properties of highly filled polymer materials at extrusion conditions, because they are very similar to their manufacturing conditions in practise. Online rheometry is proposed to be the most accurate way to measure such properties (Steffe, 1996), while the extrusion with an offline approach still remains challenging to achieve. Capillary and slit die geometries are the most widely used types of the rheometers which are mounted at the outlet of extruders to measure the rheological behaviour of melted materials online. Slit die geometries are mostly preferred for online measurements, because the mounted pressure transducers allow measuring the pressure directly on the input and on the output of the flow channel without any disturbance of the flow. Considering this fact, the slit die was selected as an appropriate geometry for measuring the rheological behaviour of PIM materials.

The rheological properties determined from the slit die rheometer are in a good agreement with those from the capillary rheometer. This fact has already been demonstrated by Han (1971) who measured the flow behaviour of polymeric materials, namely high-density polyethylene, low-density polyethylene, polypropylene, and polystyrene, using two rectangular slit dies with aspect ratios of 10 and 20. Recently Horvat et al. (2013) attached an online slit die rheometer to the exit of a high speed twin screw extruder to measure rheological properties of plasticized starch based melts like wheat flour and corn grits.

The flow of highly filled polymer melts is accompanied with the occurrence of wall slip in both rotational and capillary rheometers. In processing of PIM compounds the wall slip is a desirable effect and need to be characterized, not eliminated, because the simulations of the continuous processing of highly filled suspensions especially require the incorporation of their wall slip behaviour into the analysis in order to indicate and eliminate the phase separation of the individual components. Slit die as an alternative geometry to the parallel-plate disks enhances the wall-slip effect, because there is a shear-stress gradient present during the flow.

In this thesis four types of slit die with different size parameters and different roughness profiles of the flow channel were used for investigation of wall-slip effect of PIM materials. As mentioned in section 3.1, smooth walls of the flow channel and small geometry size are one of the parameters, which give rise to wall-slip depletion (Barnes, 1995). This fact was considered when selecting the appropriate geometry size and

roughness. The roughness of the channel surfaces was adjusted, because even for rheologically simpler materials as pure polymer melts the surface of the walls plays a significant role in controlling the wall-slip behaviour and its elimination. For a simple description, the surfaces will be marked as a smooth and a roughened. The geometries used for measurements were following:

- Slit die with parameters (15/1/100) mm, smooth surface
- Slit die with parameters (15/1/100) mm, roughened surface
- Slit die with parameters (10/0.5/100) mm, smooth surface
- Slit die with parameters (10/0.5/100) mm, roughened surface

where the parameter  $H/W/L$  indicates the ratio of the height  $H$  to width  $W$  to length  $L$  of slit die channel. As an example, the profile of slit die flow channel with roughened surface and parameters (15/1/100) mm is shown in Fig. 16.



*Fig. 16. Representation of slit die geometry with parameters (15/1/100) mm and roughened surface*

### **6.3 Slit die roughness measurements**

The measurements of roughness surface of the slit die channels with the use of Mitutoyo SJ-301 device have been done for all used geometries. The flow channel surfaces were compared by means of roughness profile  $R_a$  ( $\mu\text{m}$ ), which is by far the most common parameter for determining the quality of surface topography. It is arithmetical average of the sums of all profile values from the mean line. The other two parameters  $R_z$  and  $R_{mr}$  were also measured.  $R_z$  ( $\mu\text{m}$ ) is maximum height of the roughness profile and is calculated as a

sum from the height of the highest profile peak and the depth of the lowest profile valley within a sampling length  $l_r$ . Material proportion of the profile  $R_{mr}$  (%) is the quotient from the sum of all material lengths of the profile elements at the specified section height  $c$  and the measured length  $l_r$ .

The roughness profile values were measured in both longitudinal and transverse direction. Tables 5, 6, 7 and 8 sufficiently describe the differences in surface roughness of all dies employed.

*Table 5 The roughness parameters of smooth and roughened (10/0.5/100) mm slit die channels in longitudinal direction*

Slit die (10/0.5/100) mm _ longitudinal direction							
Smooth				Roughened			
	$R_a$ [ $\mu\text{m}$ ]	$R_z$ [ $\mu\text{m}$ ]	$R_{mr}$ [50%]		$R_a$ [ $\mu\text{m}$ ]	$R_z$ [ $\mu\text{m}$ ]	$R_{mr}$ [50%]
$X_1$	0.22	1.9	6	$X_1$	0.75	3.67	35
$X_2$	0.21	1.33	36	$X_2$	0.75	3.67	52
$X_3$	0.18	1.6	20	$X_3$	0.82	3.95	37
$X_4$	0.2	1.1	9	$X_4$	0.61	3.33	27
$X_5$	0.15	0.96	14	$X_5$	0.82	3.76	41
$X_6$	0.11	0.91	7	$X_6$	0.57	2.86	41
$X_7$	0.15	0.95	3	$X_7$	0.54	3.1	73
$X_8$	0.26	1.47	21	$X_8$	0.55	3.14	26
$X_9$	0.22	1.36	5	$X_9$	0.57	2.89	66
$X_{10}$	0.2	1.13	14	$X_{10}$	0.73	3.64	36
$\bar{X} \pm u_A$	<b>0.19 ± 0.014</b>	<b>1.2 ± 0.081</b>	<b>13.5 ± 3.2</b>	$\bar{X} \pm u_A$	<b>0.67 ± 0.036</b>	<b>3.40 ± 0.12</b>	<b>43.4 ± 5.0</b>

Parameter  $u_A$  the standard uncertainty of type A, which is determined from the results of repeated measurements by statistical analysis of a series of measured values as in the case of random measurements errors. They are caused by unknown effects and their values decline with the number of measurements.

Table 6 The roughness parameters of smooth and roughened (10/0.5/100) mm slit die channels in transverse direction

Slit die (10/0.5/100) mm _ transverse direction							
Smooth				Roughened			
	$R_a$ [ $\mu\text{m}$ ]	$R_z$ [ $\mu\text{m}$ ]	$R_{mr}$ [50%]		$R_a$ [ $\mu\text{m}$ ]	$R_z$ [ $\mu\text{m}$ ]	$R_{mr}$ [50%]
$X_1$	0.15	0.86	52	$X_1$	0.91	4.61	31
$X_2$	0.32	2.26	46	$X_2$	0.98	5.12	45
$X_3$	0.3	1.64	16	$X_3$	0.82	4.17	24
$X_4$	0.2	1.49	27	$X_4$	0.97	4.89	52
$X_5$	0.3	2.4	9	$X_5$	1.5	5.29	57
$X_6$	0.39	2.52	19	$X_6$	1.1	4.87	55
$X_7$	0.2	1.31	71	$X_7$	1.3	5.13	45
$X_8$	0.19	1.17	78	$X_8$	0.87	4.22	37
$X_9$	0.12	0.7	30	$X_9$	0.96	4.52	39
$X_{10}$	0.33	2.16	39	$X_{10}$	0.94	5.7	40
$\bar{X} \pm u_A$	<b>0.25 <math>\pm</math> 0.028</b>	<b>1.62 <math>\pm</math> 0.195</b>	<b>38.7 <math>\pm</math> 7.3</b>	$\bar{X} \pm u_A$	<b>0.95 <math>\pm</math> 0.023</b>	<b>4.79 <math>\pm</math> 0.124</b>	<b>42.5 <math>\pm</math> 3.3</b>

Table 7 The roughness parameters of smooth and roughened (15/1/100) mm slit die channels in longitudinal direction

Slit die (15/1/100) mm _ longitudinal direction							
Smooth				Roughened			
	$R_a$ [ $\mu\text{m}$ ]	$R_z$ [ $\mu\text{m}$ ]	$R_{mr}$ [50%]		$R_a$ [ $\mu\text{m}$ ]	$R_z$ [ $\mu\text{m}$ ]	$R_{mr}$ [50%]
$X_1$	0.06	0.49	91	$X_1$	0.75	3.86	22
$X_2$	0.05	0.42	98	$X_2$	0.89	4.56	20
$X_3$	0.08	0.53	94	$X_3$	0.63	3.33	20
$X_4$	0.07	0.57	25	$X_4$	0.74	3.96	39
$X_5$	0.07	0.43	59	$X_5$	0.85	5.14	27
$X_6$	0.07	0.59	14	$X_6$	0.94	4.36	39
$X_7$	0.07	0.44	51	$X_7$	0.66	3.88	22
$X_8$	0.06	0.41	86	$X_8$	0.7	3.89	21
$X_9$	0.08	0.5	46	$X_9$	0.74	4.4	27
$X_{10}$	0.07	0.51	68	$X_{10}$	0.81	4.13	47
$\bar{X} \pm u_A$	<b>0.07 <math>\pm</math> 0.003</b>	<b>0.49 <math>\pm</math> 0.02</b>	<b>63.2 <math>\pm</math> 9.3</b>	$\bar{X} \pm u_A$	<b>0.77 <math>\pm</math> 0.032</b>	<b>4.12 <math>\pm</math> 0.154</b>	<b>28.4 <math>\pm</math> 3.1</b>

Table 8 The roughness parameters of smooth and roughened (15/1/100) mm slit die channels in transverse direction

Slit die (15/1/100) mm _ transverse direction							
Smooth				Roughened			
	$R_a$ [ $\mu\text{m}$ ]	$R_z$ [ $\mu\text{m}$ ]	$R_{mr}$ [50%]		$R_a$ [ $\mu\text{m}$ ]	$R_z$ [ $\mu\text{m}$ ]	$R_{mr}$ [50%]
$X_1$	0.12	1	98	$X_1$	1.14	5.31	37
$X_2$	0.11	0.81	86	$X_2$	0.93	4.57	49
$X_3$	0.17	1.21	99	$X_3$	1.1	5.53	33
$X_4$	0.13	1.25	93	$X_4$	1.6	5.91	8
$X_5$	0.17	1.9	89	$X_5$	0.92	4.43	46
$X_6$	0.13	1.5	98	$X_6$	0.93	4.83	52
$X_7$	0.19	1.42	91	$X_7$	0.78	4.31	65
$X_8$	0.19	1.27	99	$X_8$	0.76	4.27	47
$X_9$	0.1	0.85	97	$X_9$	0.94	4.61	43
$X_{10}$	0.2	1.51	99	$X_{10}$	0.84	4.41	47
$\bar{X} \pm u_A$	<b>0.15 <math>\pm</math> 0.012</b>	<b>1.15 <math>\pm</math> 0.072</b>	<b>94.9 <math>\pm</math> 1.5</b>	$\bar{X} \pm u_A$	<b>0.94 <math>\pm</math> 0.041</b>	<b>4.82 <math>\pm</math> 0.180</b>	<b>42.7 <math>\pm</math> 4.7</b>

## 6.4 Rheology

The characterization of the flow behaviour of highly filled polymer materials is complicated by the occurrence of wall slip, and in many cases a number of solutions have been developed to eliminate this phenomenon. However, in the case of measurements for this thesis the wall slip is a desirable effect, because the creation of a thin polymer layer on the wall prevents the separation of binder and filler components during the processing of PIM materials, mainly in the region of high deformation rates. Considering wall-slip conditions, there appears to be no shear-rate gradient in the middle of the velocity profile, thus the solid particles do not tend to move away from the inner core towards the walls, and no separation from the polymer matrix occurs. Regarding the wall-slip effect and its impact on the rheological behaviour of selected feedstock, several factors have been taken into account such as the geometry parameters, surface roughness of the flow channels, the influence of powder and polymer components, and also the impact of pressure conditions on the flow behaviour.

In order to study the wall-slip behaviour of selected materials the shear flow properties at screw speeds of up to maximum 100 rpm were measured with the online rheometer at temperatures recommended by the manufacturers in the material data sheets. The extruded samples were taken away from the extrusion die at intervals which varied according to the

screw speed. The samples were then weighed and the shear stress  $\tau$  and the shear rate  $\dot{\gamma}$  necessary for the construction of flow curve were evaluated as follows:

Firstly, the volumetric flow rate  $\dot{Q}$  ( $\text{mm}^3/\text{s}$ ) is calculated from the Eq. (3):

$$\dot{Q} = \frac{V}{t} \quad (3)$$

where  $V$  ( $\text{mm}^3$ ) is the volume of the fluid which passes through a given surface per unit time  $t$  (s). Volume of extruded sample can be easily calculated as its weight divided by density.

The shear stress  $\tau$  (Pa) corrected by the use of Bagley-pressure correction is calculated by the measured pressure drop  $\Delta p$  at a certain volumetric flow rate  $\dot{Q}$  according to Eq. (4):

$$\tau = \frac{(p_5 - p_3) \cdot H}{2L} \quad (4)$$

where  $p_5$  (Pa) is the pressure value on the inlet of the flow channel,  $p_3$  (Pa) is the pressure on the outlet of the channel,  $H$  (mm) represents the height of the slit die and  $L$  (mm) is the length between pressure transducers  $p_3$  and  $p_5$ .

Then, the apparent shear rate  $\dot{\gamma}_a$  (1/s) is computed from the Eq. (5) shown below:

$$\dot{\gamma}_a = \frac{6 \cdot \dot{Q}}{H^2 \cdot W} \quad (5)$$

where  $W$  (mm) indicates the width of slit geometry, respectively. Apparent shear rate  $\dot{\gamma}_a$  in the relation means that there are some assumptions made in order to calculate its value, especially Newtonian behaviour of the fluid. Consequently, to obtain the true value of the shear rate  $\dot{\gamma}$ , Rabinowitsch correction would have to be applied:

$$\dot{\gamma}_a = \frac{6 \cdot \dot{Q}}{H^2 \cdot W} \cdot \frac{3n+1}{4n} \quad (6)$$

where  $n$  (-) is the index of non-Newtonian behaviour, and can be calculated from the slope of log-log plot of the true shear stress  $\tau$  versus apparent shear rate  $\dot{\gamma}_a$  using Eq. (7):

$$n = \frac{\partial(\log\tau)}{\partial(\log\dot{\gamma}_a)} \quad (7)$$

The flow curves of individual materials processed on the online rheometer were evaluated from measured data with the help of the equations above, and they describe the dependence of shear stress on the apparent shear rate.

PolyMIM 17-4PH feedstock was processed at following zone temperatures: 170, 180, 185, 190, 190 °C. The first three temperatures were set for the extrusion screw, and the last two corresponds to zones at the slit die. The flow curves for (15/1/100) mm (Fig. 17) and (10/0.5/100) mm slit die (Fig. 18) were evaluated from measured data. As can be seen, the rheological behaviour of PolyMIM 17-4PH material is dependent on the surface roughness of flow channel. This is a kind of an indication that the wall slip is present during the processing of this material because using of roughened surface slit die causes the elimination of slipping on the walls, and thus the higher values of shear stress are obtained. The effect of roughness is evident for both slit die geometries.

PolyMIM 17-4PH was also the only material tested on the impact of pressure conditions on material viscosity. The pressure applied on the polymer melt was controlled by the setting of movable valve. The fully-open position responded to the smallest pressure and by closing of the valve the pressure was gradually enhanced. Figures 17 and 18 show the influence of valve positions on the shear stress. While the flow behaviour is almost independent on pressure conditions for smooth slit die, the variation of pressure growth with the use of roughened slit die has stronger impact on shear viscosity and the flow curve moves towards higher values of shear stress by closing of moveable valve. The shear stress values increase with enhancing the pressure on the material. Based on this fact, the study of further materials continued with the measurements using only the open position of the movable valve.



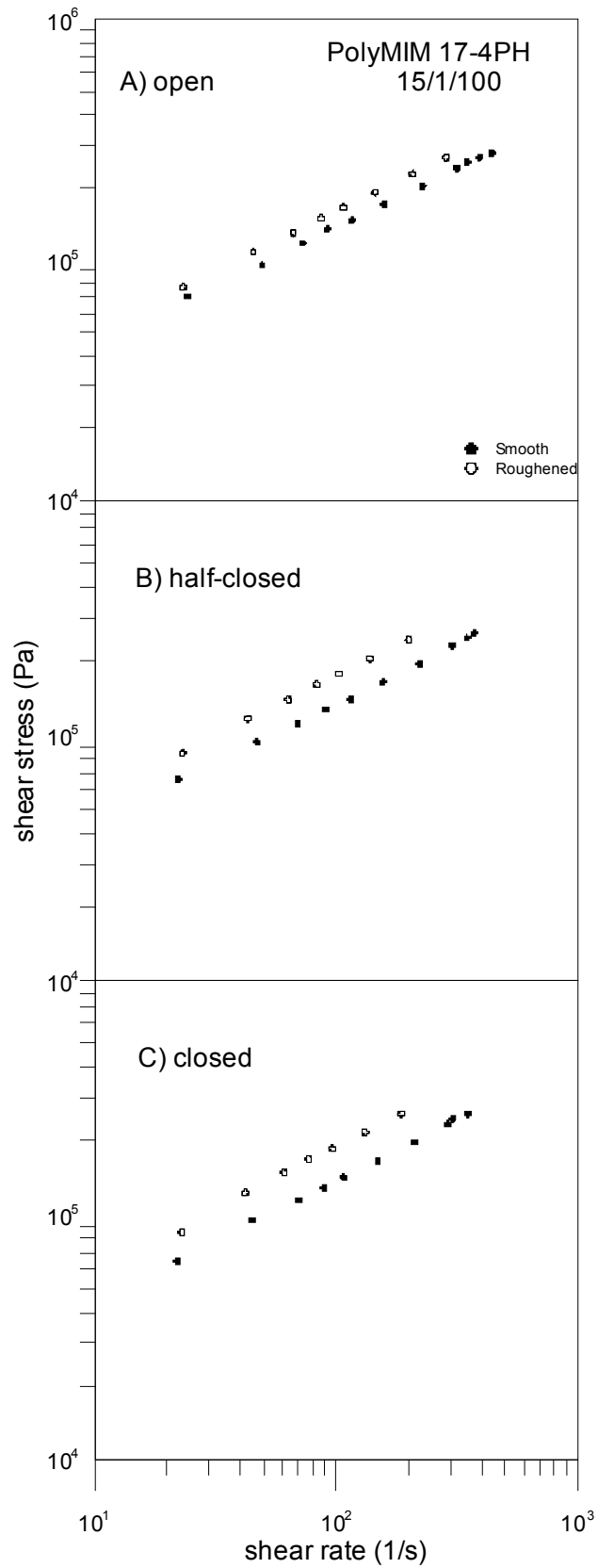
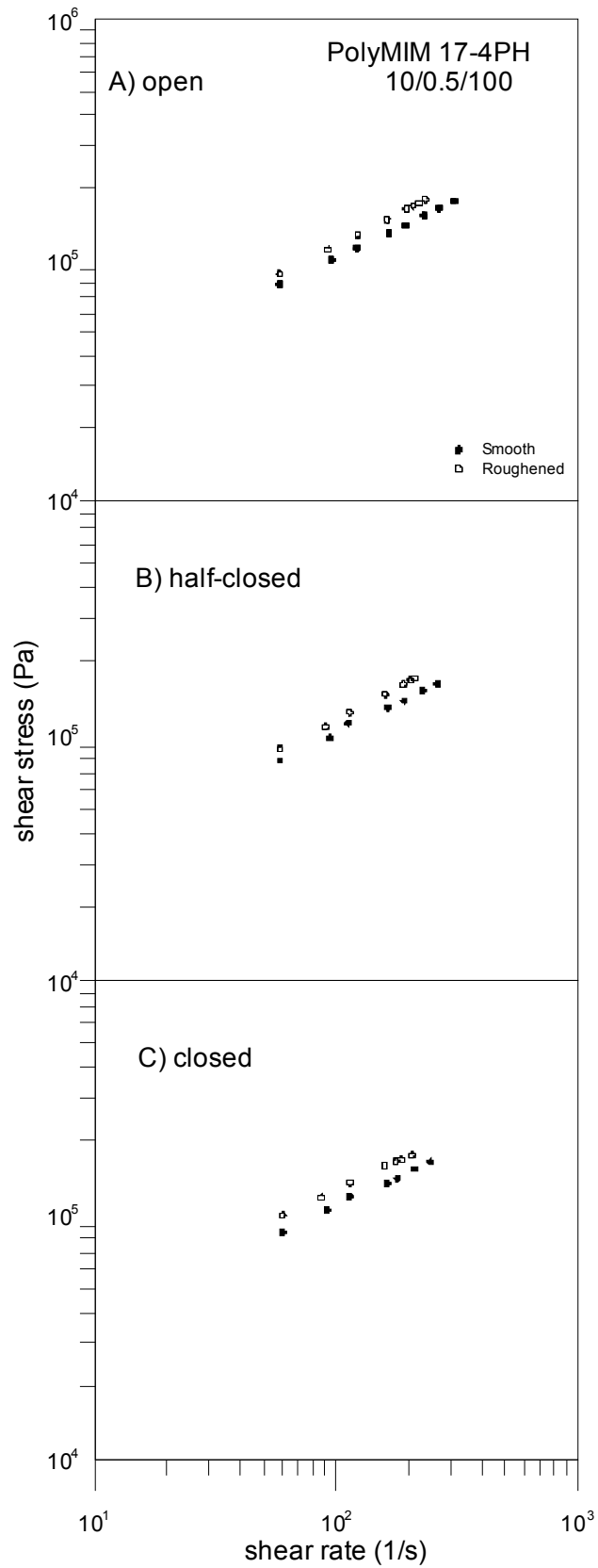


Fig. 17. Shear stress as a function of shear rate for PolyMIM 17-4PH feedstock extruded through smooth and roughened slit die with parameters (15/1/100) mm. The position of movable valve was (A) open, (B) half-closed and (C) closed



*Fig. 18. Shear stress as a function of shear rate for PolyMIM 17-4PH feedstock extruded through smooth and roughened slit die with parameters (10/0.5/100) mm. The position of movable valve was (A) open, (B) half-closed and (C) closed*

The screw speeds applied on slit die with smooth surface were slightly higher than those applicable for roughened slit die because the pressure occurring during processing was lower. It is more evident for slit die with parameters (10/0.5/100) mm, which has smaller cross-section than (15/1/100) mm slit die. Not only PolyMIM 17-4PH, but all measured feedstocks revealed this behaviour.

The rheological behaviour of PolyMIM 316L feedstock was measured at temperatures: 180, 185, 190, 190, 190 °C, which differed from those used for PolyMIM 17-4PH only in zones of the extrusion part. The temperatures on slit die were the same for both materials. Comparing to 17-4PH composition, where slip is evident, the flow curves evaluated from measured data are almost identical for the same geometry and no influence of surface roughness on the flow of this material is seen either for (15/1/100) mm (Fig. 19) or for (10/0.5/100) mm geometry (Fig. 20). However, there is a noticeable difference between the indexes of non-Newtonian behaviour obtained for roughened slit die, which will be further described in section below.

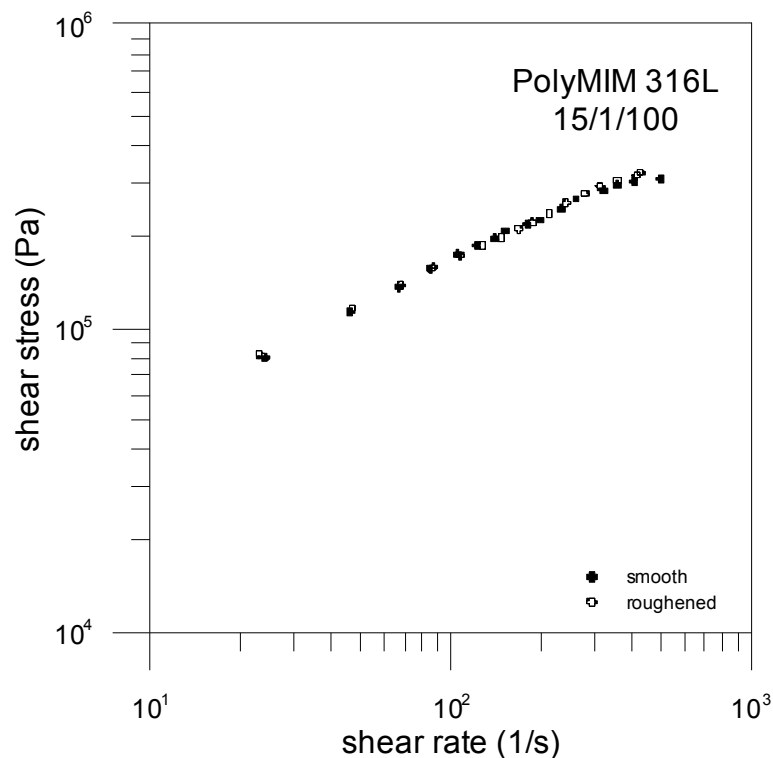


Fig. 19. Shear stress as a function of shear rate for PolyMIM 316L feedstock extruded through smooth and roughened slit die with parameters (15/1/100) mm and open position of movable valve

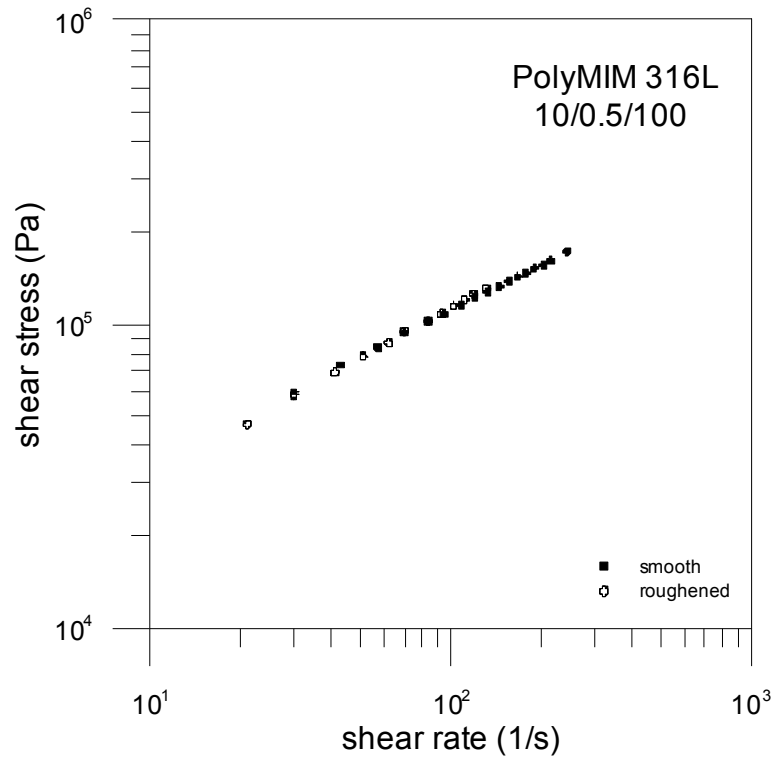


Fig. 20. Shear stress as a function of shear rate for Catamold 316L feedstock extruded through smooth and roughened slit die with parameters (10/0.5/100) mm and open position of movable valve

The most important thing which needs to be considered when determining the presence of the wall slip for the individual materials is the influence of geometry parameters on the rheological behaviour. The impact of slit die parameters on the flow behaviour is shown for PolyMIM 17-4PH (Fig. 21) and PolyMIM 316L (Fig. 22) feedstocks with the use of both smooth and roughened slit die. If no slipping on the wall was present, the shear viscosity/stress would be independent of the geometry parameters. However, it is obvious, that wall-slip effect occurs in the whole shear-rate profile for both materials. It can be seen, that shear stress and apparent shear viscosity of both feedstocks are higher at (15/1/100) mm geometry than with the use of (10/0.5/100) mm geometry.

According to Eq. (4), the height reduction of slit die should lead to increase of measured pressure to observe the same values of the shear stress and apparent shear viscosity of liquid. The experimental measurements proved that by using slit die with lower height (0.5 mm) the higher pressures were achieved, thus slightly lower speed of extrusion screw could be applied than at slit die with the height of 1 mm.

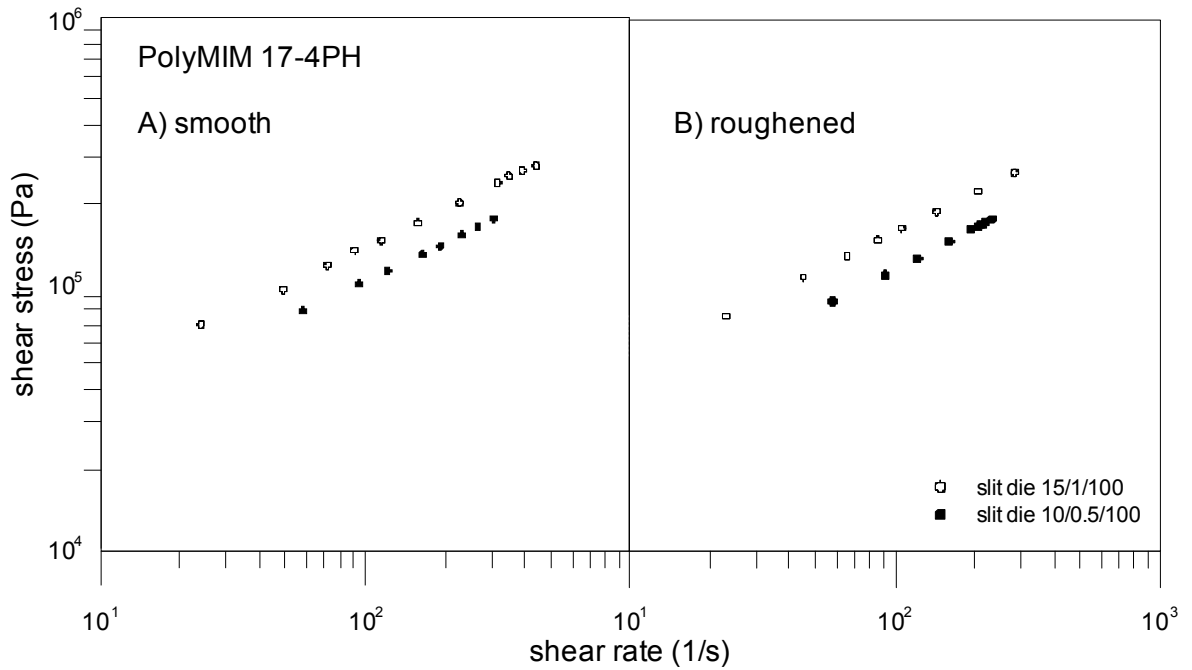


Fig. 21. The influence of slit die parameters on the rheological behaviour of PolyMIM 17-4PH feedstock for (A) smooth or (B) roughened surface slit die

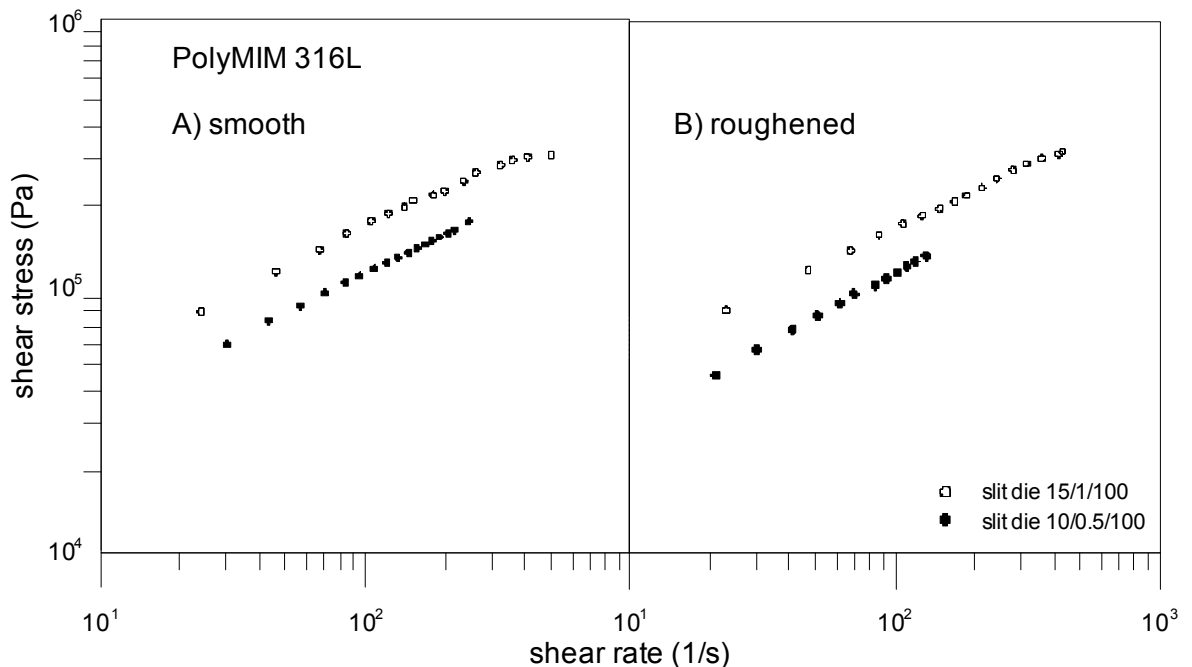


Fig. 22. The influence of slit die parameters on the rheological behaviour of PolyMIM 316L feedstock for (A) smooth or (B) roughened surface slit die

When comparing the rheological behaviour of PolyMIM 17-4PH and PolyMIM 316L feedstocks the influence of the powder composition should be noted. Both materials had

the same characteristic of polymer binder but differed in the composition of metal powder (stainless steel type 17-4PH or type 316L). It can be seen from Fig. 23, that these materials show very similar flow behaviour when processed through roughened slit die. It is also obvious that the difference in flow curves rise with the use of smooth surface slit die. The shear stress values obtained for feedstock which contains 17-4PH metal powder are lower than those for feedstock with 316L powder composition.

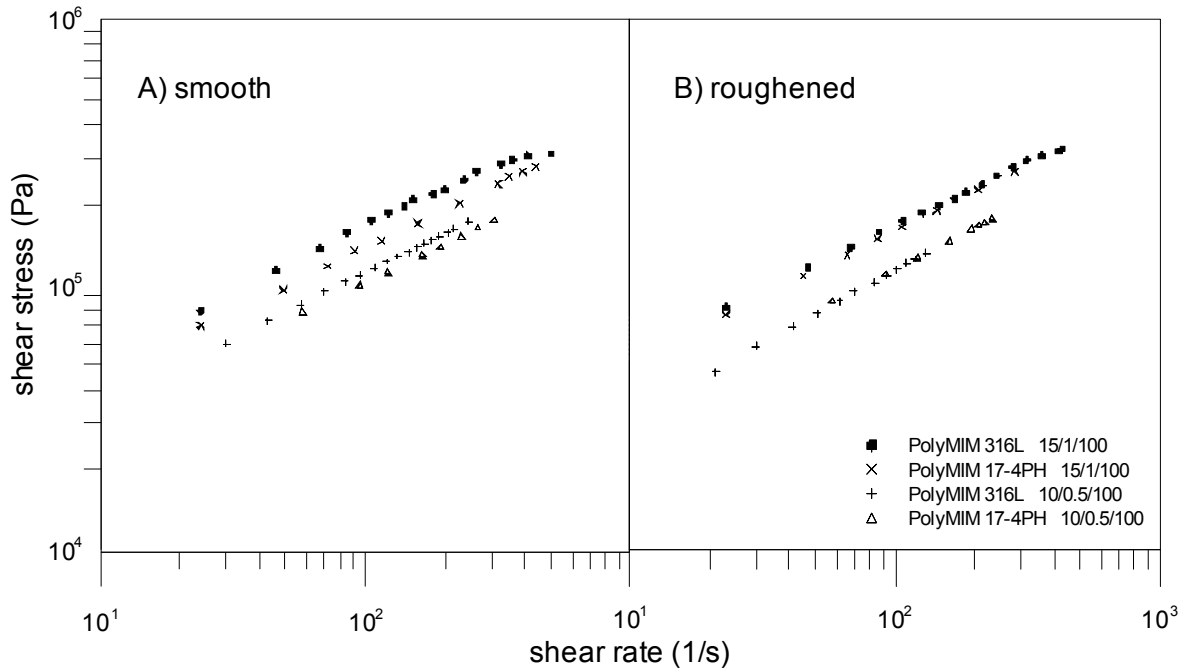


Fig. 23. Influence of the powder composition on the rheological behaviour of PolyMIM 17-4PH and PolyMIM 316L feedstocks for (A) smooth or (B) roughened slit die

The processing temperatures of Catamold 316L feedstock were following: 160, 170, 180, 190, 190 °C. The temperature set for slit die was again 190 °C, the same as for the previous materials. As shown in Fig. 24, Catamold 316L feedstock exhibited an interesting rheological behaviour. There is an effect of slit die roughness seen at shear rates lower than  $10^2 \text{ s}^{-1}$ , which reduces gradually to total extinction. Also the indexes of non-Newtonian behaviour ( $n$ ) are dependent on the values of shear rate and there is an evident change in the flow behaviour. The values of  $n$  is 0.80 for smooth surface and 0.77 for roughened surface. In the case of smooth slit die the material behaves almost as a Newtonian fluid at shear rates lower than  $10^2 \text{ s}^{-1}$  ( $n = 0.98$ ), but increasing the shear rates causes that the flow is changed to more pseudoplastic ( $n = 0.72$ ). However, the index of non-Newtonian behaviour calculated for the whole range of shear rates has the value of 0.80. The change in the slope of the flow curve can be also seen for roughened slit die.

Firstly, the material exhibits a behaviour with  $n$  value of 0.94, which is changed to more pseudoplastic one at the shear rates higher than  $10^2 \text{ s}^{-1}$  ( $n = 0.68$ ). The flow curves were only constructed from data measured on slit die with parameters (15/1/100) mm because the measurements with use of (10/0.5/100) mm slit die geometry could not be carried out for this material, and no appropriate data for the construction of flow curve was obtained. It was repeatedly and unsuccessfully measured three times with the properly controlled measuring conditions, however the pressure at the inlet to the flow channel was too high and control pressure sensor p<sub>6</sub> showed maximum allowed value (700 bar). Thus the measurements had to be always stopped at screw speed of 4 rpm and the material could not be processed because of the limit of control pressure transducer. Even when the temperature in the third zone of extrusion machine was increased the situation remained the same. Thus it was not possible to compare different size geometries and determine the wall-slip phenomenon. This problem could be sorted by using the control sensors, which would allow us to apply higher pressure than 700 bar.

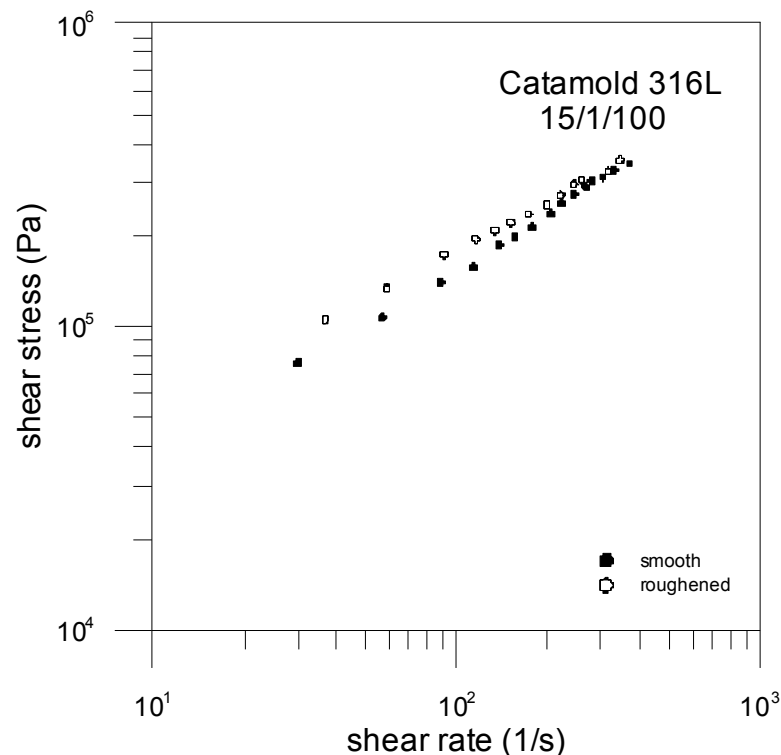


Fig. 24. Shear stress as a function of shear rate for Catamold 316L feedstock extruded through smooth and roughened slit die with parameters (15/1/100) mm and open position of movable valve

PolyMIM 316L and Catamold 316L feedstocks contain the same metal powder component, but varied in the binder composition. According to the rheological behaviour of these

materials, different polymer binder caused a significant change in plasticity and indexes of non-Newtonian behaviour.

Embemold 17-4PH was processed at temperatures 110, 120, 130, 150, 150 °C, which were significantly lower than temperatures used for the other materials. It has already been proved in the previous measurements on capillary rheometers that it is not possible to derive the flow curves of this material because it exhibits the plastic flow behaviour and slips on the walls of flow channel. With the increase of the processing temperature, the material would only show more plasticity. According to the measurements, Catamold 17-4PH is not suitable for processing on the online rheometer Brabender Extrusiograph 19/25D with slit die channels with ratio of 15/1 or 10/0.5. The maximum pressure value obtained at the screw speeds of 100 rpm was 25 bar. Due to the plastic flow, the pressure transducers registered only very low values of pressure in comparison to other materials. Generally the plastic deformation is dependent on the deformation speed, so higher shear rates should be applied to increase the shear stresses. Thus Embemold 17-4PH feedstock would be more appropriate for injection moulding process, where higher shear rates are applied.

Although all investigated PIM feedstocks are classified as highly filled materials, they exhibited the behaviour of pseudoplastic fluids, which is typical for pure polymer melts. The pseudoplastic fluids are characterized by a decrease in apparent viscosity with increasing shear stress. Pseudoplastic behaviour can be directly seen from the slope of flow curves, and is also confirmed by the values of the indexes of non-Newtonian behaviour  $n$  (Fig. 9), which are lower than 1.

It can be seen from Table 9 that non-Newtonian indexes of PolyMIM 17-4PH differ according to the size and surface roughness of used slit die and the position of movable valve. The indexes calculated for slit die with parameters (15/1/100) mm and roughened surface are strongly dependent on the position of movable valve. The index  $n$  increases with moving the valve towards the closed position and has the value of 0.59 for open position, 0.74 for half-closed position and 0.81 for fully-closed position. On the other hand  $n$  for roughened slit die with parameters (10/0.5/100) mm are almost independent on the position of valve. They have the values of 0.53 for open position, 0.54 for half-closed position and 0.56 for closed position. Also the indexes  $n$  determined for smooth surface slit



die with parameters either (15/1/100) mm or (10/0.5/100) mm do not differ so much depending on the position of movable valve and their values are shown in Table 9.

When comparing the non-Newtonian indexes of PolyMIM 316L the values obtained for roughened slit dies – 0.57 for (15/1/100) mm and 0.75 for (10/1/100) mm geometry – should be noted as there is a rather large difference between them. By contrast, the indexes  $n$  determined for smooth surface channel are rather similar with values of 0.48 for (15/1/100) mm slit die and 0.51 for (10/0.5/100) mm slit die.

As shown in Table 9 the indexes of non-Newtonian behaviour of Catamold 316L calculated for smooth and roughened slit die have rather close values – 0.80 for smooth and 0.77 for roughened surface.

*Table 9 Indexes of non-Newtonian behaviour calculated for the individual materials*

Material	Die parameters (mm)	Surface	Position	$n$ (-)
PolyMIM 17-4PH	15/1	smooth	open	0.39
		roughened	open	0.59
		smooth	half-closed	0.44
		roughened	half-closed	0.74
		smooth	closed	0.47
		roughened	closed	0.81
	10/0.5	smooth	open	0.38
		roughened	open	0.53
		smooth	half-closed	0.40
		roughened	half-closed	0.54
		smooth	closed	0.41
		roughened	closed	0.56
PolyMIM 316L	15/1	smooth	open	0.48
		roughened	open	0.57
	10/0.5	smooth	open	0.51
		roughened	open	0.75
Catamold 316L	15/1	smooth	open	0.80
		roughened	open	0.77

## 6.5 Structure analyses

The dependence of rheological behaviour on geometry size was the most evident for PolyMIM 17-4PH. Accordingly, this material was selected for analyzing the surface structure of samples. SEM analysis of samples extruded through smooth and roughened slit die with parameters (10/0.5/80) mm was done by taking images of samples processed at four different screw speeds (3, 5, 10, 15 rpm). The pictures were taken at magnification 200x (Fig. 25) and 500x (Fig. 26).

It is distinct from figures that the influence of surface roughness increased with the increase of screw speed. There is not a big difference in images taken from samples extruded at speed of 3 rpm, and the surfaces seem to be the same. The influence of roughness started to manifest only at screw speed of 5 rpm, where the surface of sample extruded through roughened slit die is more roughened than the surface of smooth sample. The difference in effect of smooth and roughened surface is the most evident at speed of 15 rpm. The large holes were created on the surface of samples extruded through roughened slit die at this speed. However, there are not evident such holes and plucked places on the smooth samples.

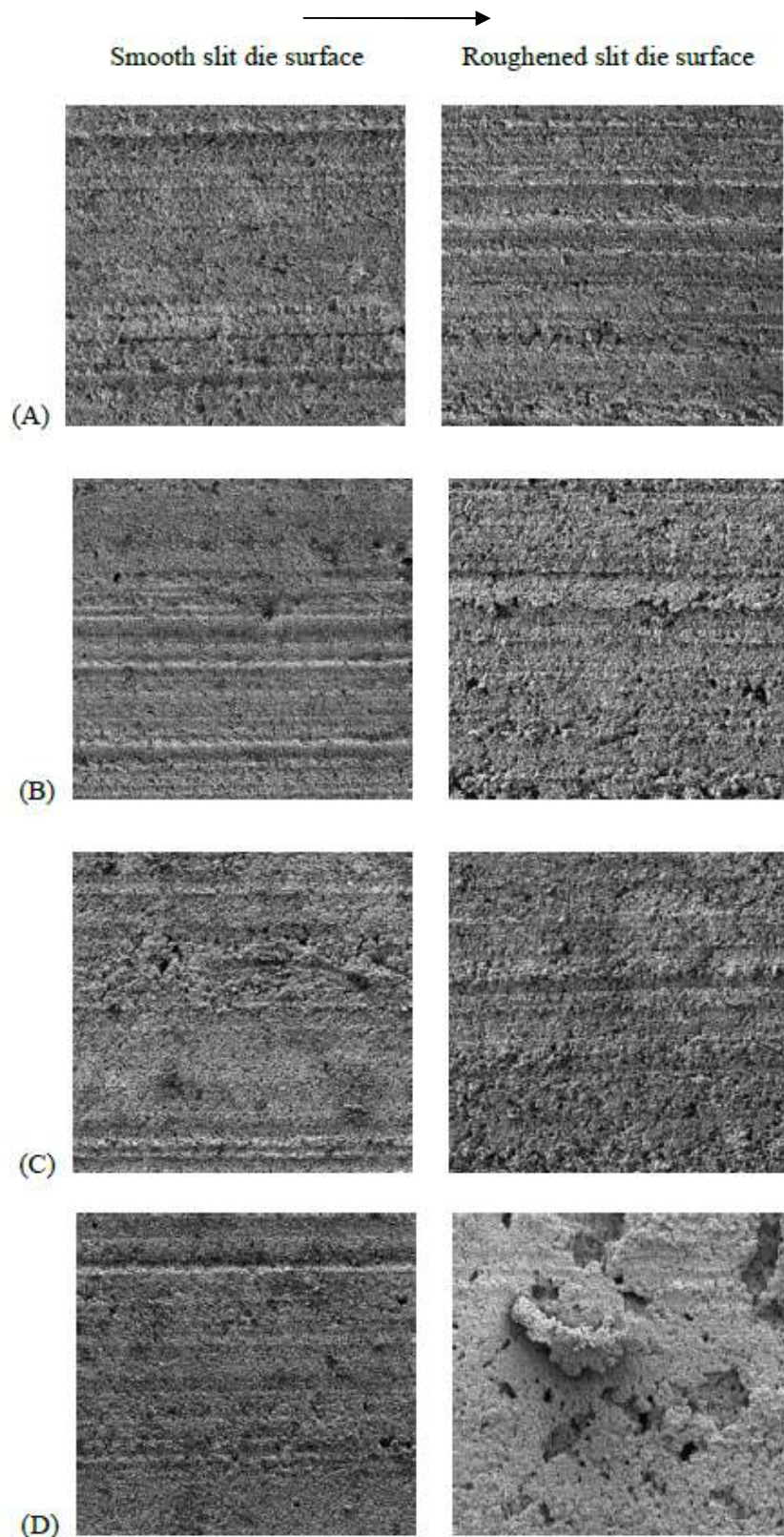


Fig. 25. SEM images of polyMIM 17-4PH samples extruded through smooth and roughened slit die with (10/0.5/100) mm parameters at speeds (A) 3 rpm (B) 5 rpm (C) 10 rpm (D) 15 rpm (magnification 200x). The arrow shows the direction of the flow

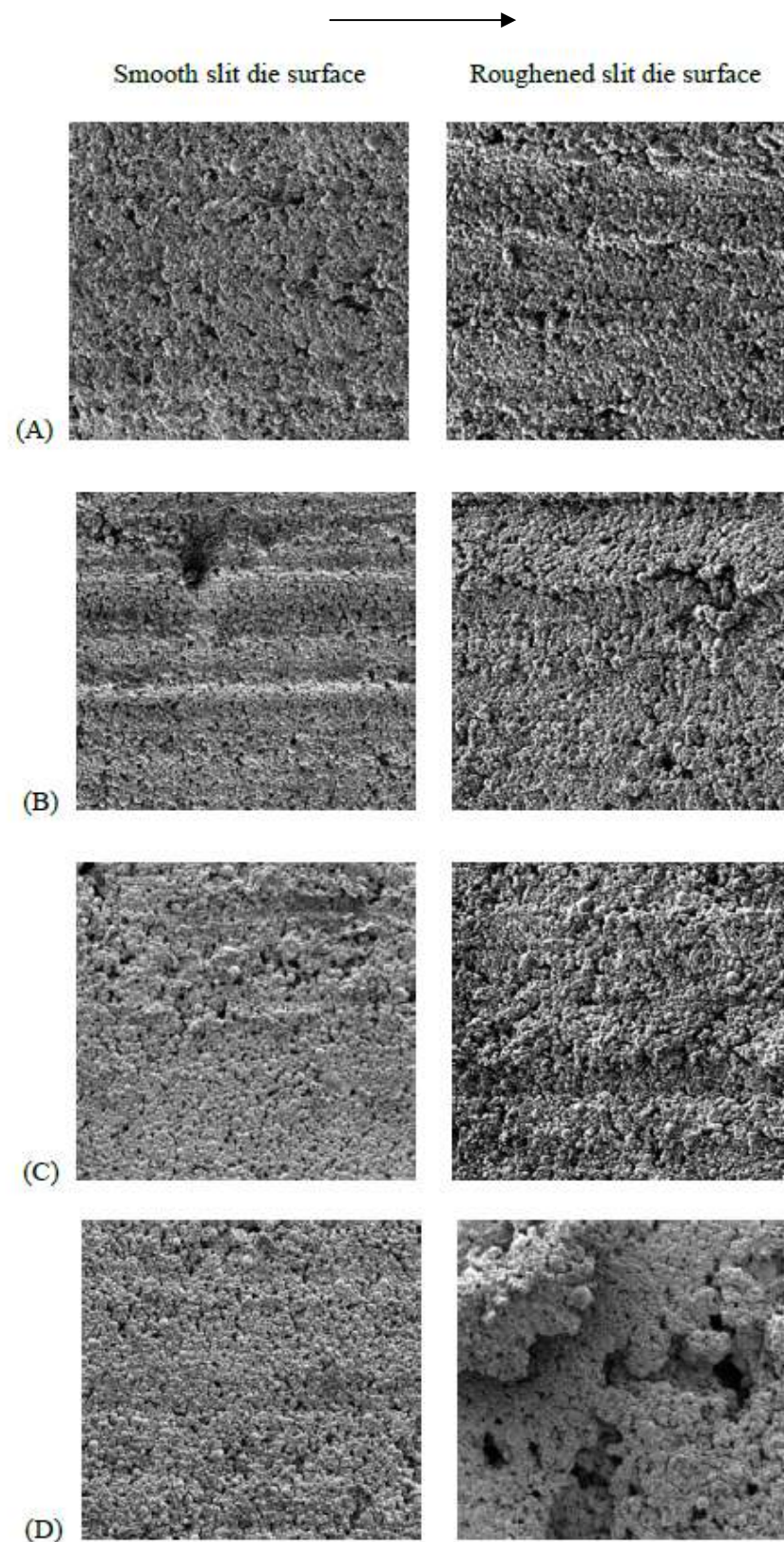
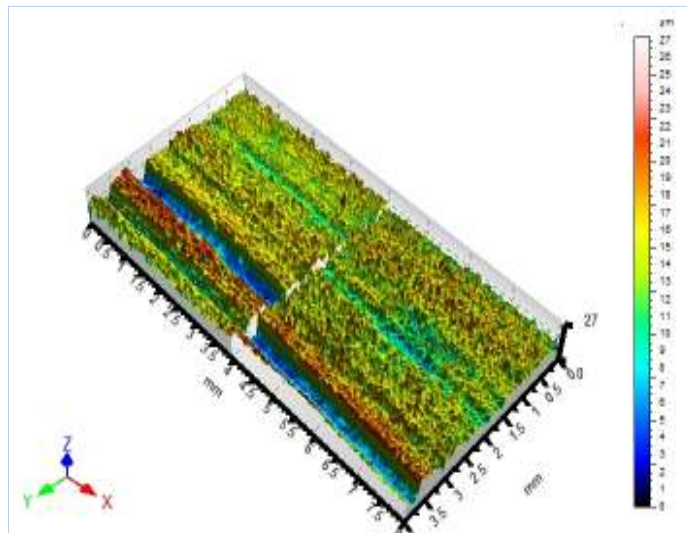


Fig. 26. SEM images of polyMIM 17-4PH samples extruded through smooth and roughened slit die with (10/0.5/100) mm parameters at speeds (A) 3 rpm (B) 5 rpm (C) 10 rpm (D) 15 rpm (magnification 500x). The arrow shows the direction of the flow

Contactless surface analysis was selected as an appropriate method for characterization both smooth and roughened surfaces of samples in more details and their representation in 3D view. The samples of PolyMIM 17-4PH extruded at the same screw speeds as SEM samples were used for this analysis. The surface roughness of individual samples was compared according to parameter  $R_z$ . As well as SEM analysis this method also confirms the increasing of influence of the surface roughness with increasing the screw speed.

It can be seen from Fig. 27 that there is not a big difference in two samples extruded through a smooth and a roughened slit die at speed of 3 rpm and roughness profiles are rather similar with close  $R_z$  values. It was evaluated from the measurements that  $R_z$  for roughened surface sample was 33  $\mu\text{m}$  and 29  $\mu\text{m}$  for smooth sample.



*Fig. 27. Surface analysis of PolyMIM 17-4PH samples extruded through smooth (left) and roughened (right) (10/0.5/100) mm slit die at speed 3 rpm*

The surfaces of PolyMIM 17-4PH samples extruded through a smooth and a roughened slit die at speed 5 rpm are compared in Fig. 28. There is a significant difference in surface roughness with value of  $R_z$  33  $\mu\text{m}$  for smooth sample and 91  $\mu\text{m}$  for roughened sample.

The surface of samples becomes more roughened by increasing of screw speed to 10 rpm (Fig. 29). However,  $R_z$  are not different as much as at speed of 5 rpm. They have a value of 97  $\mu\text{m}$  for smooth sample and 107  $\mu\text{m}$  for roughened sample.

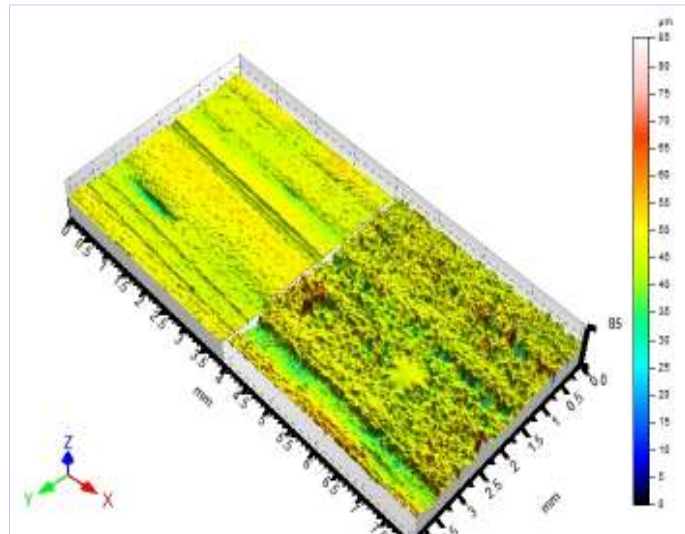


*Fig. 28. Surface analysis of PolyMIM 17-4PH samples extruded through smooth (left) and roughened (right) (10/0.5/100) mm slit die at speed 5 rpm*

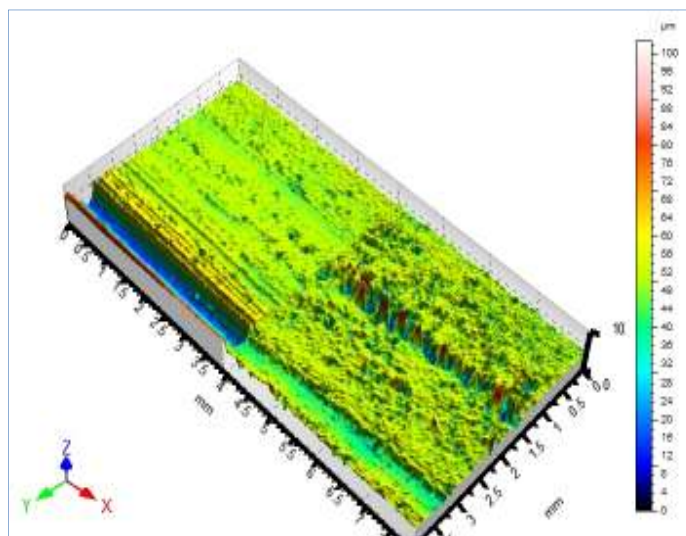


*Fig. 29. Surface analysis of PolyMIM 17-4PH samples extruded through smooth (left) and roughened (right) (10/0.5/100) mm slit die at speed 10 rpm*

Finally, the comparison of a smooth and a roughened sample extruded at speed of 15 rpm is shown in Fig. 30. It can be seen that maximum height of roughness profile is lower than for samples extruded at screw speed of 10 rpm. From the results  $R_z$  for smooth sample was 33  $\mu\text{m}$  and for roughened sample 50  $\mu\text{m}$ .

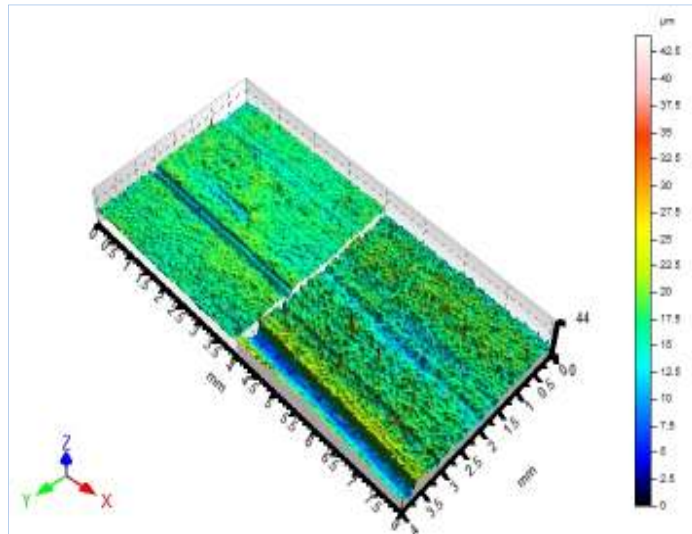


*Fig. 30. Surface analysis of PolyMIM 17-4PH samples extruded through smooth (left) and roughened (right) (10/0.5/100) mm slit die at speed 15 rpm*

## CONCLUSION

In this master thesis the rheological properties of highly filled polymer materials - PolyMIM 17-4PH, PolyMIM 316L, Catamold 316L and Embemold 17-4PH - employed in powder injection moulding were measured by means of slit die type rheometer at screw speeds typical for extrusion process. All investigated PIM feedstocks exhibited the pseudoplastic behaviour with non-Newtonian indexes lower than 1.

Firstly, the wall-slip behaviour during the processing of PolyMIM 17-4PH and PolyMIM 316L feedstocks was determined with the use of online rheometer Brabender Extrusiograph 19/25D. The influence of slit die parameters on rheological properties was proved in the whole shear-rate range for both materials. The values of shear stress and apparent shear viscosity were higher with the use of (15/1/100) mm slit die geometry than for (10/0.5/100) mm slit die. When observing the rheological behaviour of Catamold 316L the processing on (10/0.5/100) mm slit die was not possible because of the low values of control pressure transducer which allowed us only applying the maximum pressure value of 700 bar. Also the flow curves of Embemold 17-4PH could not be derived because this material exhibited the plastic behaviour and the pressure transducer registered only very low pressure values.

Beside the influence of the geometry parameters on the rheological behaviour the impact of surface roughness of the flow channel was investigated. The dependence of the flow behaviour on slit die roughness was manifested in the case of PolyMIM 17-4PH for all measurements. In contrast, PolyMIM 316L exhibited no changes in the flow curves by using the slit die channels with different surface roughness. For Catamold 316L feedstock the effect of slit die roughness could be only seen at shear rates lower than  $10^2 \text{ s}^{-1}$  and the flow curves became almost identical at higher shear rates. PolyMIM 17-4PH feedstock was also tested on the impact of pressure conditions on material viscosity by setting of the movable valve. It was found out that the values of shear stress/viscosity obtained for roughened slit die increased with enhancing the pressure on the material. Flow behaviour of the material with the use of smooth slit die was not dependent on the pressure conditions.

Further, for more detailed characterization, the surface of selected samples extruded at four different screw speeds – 3, 5, 10 and 15 rpm - were studied by means of SEM and contactless surface analysis. According to the measurements, the effect of surface roughness seen on the surface morphology of samples increased with the increasing of the



screw speed. The influence of roughness manifested itself by creation of distorted areas with holes and rougher surface of samples.

## BIBLIOGRAPHY

- Ahn, S.; Park, S. J.; Lee, S.; Atre, S. V. & German, R. M. (2009). Effect of powders and binders on material properties and molding parameters in iron and stainless steel powder injection molding process. *Powder Technology*, 193, 2, 162-169, ISSN 0032-5910
- Anonym (2007). MIM 316L stainless seeks applications in BMW Hydrogen 7 car. *PIM International*, 1, 4, 5, ISSN 1753-1497
- Barnes, H. A. & Nguyen, Q. D. (2001). Rotating vane rheometry - a review. *Journal of Non-Newtonian Fluid Mechanics*, 98, 1, 1-14, ISSN 0377-0257
- Barnes, H. A. (1995). A review of the slip (wall depletion) of polymer solutions, emulsions and particle suspensions in viscometers: its cause, character, and cure. *Journal of Non-Newtonian Fluid Mechanics*, 56, 3, 221-251
- Berginc, B.; Kampus, Z. & Sustarsic, B. (2007). Influence of feedstock characteristics and process parameters on properties of MIM parts made of 316L. *Powder Metallurgy*, 50, 2, 172-174, ISSN 0032-5899
- Cohen, Y. & Metzner, A. B. (1982). Adsorption effects in the flow of polymer solutions through capillaries. *Macromolecules*, 15, 5, 1425-1429, ISSN 0024-9297
- Cullen, P. J.; O'Donnell, C. P. & Houska, M. (2003). Rotational rheometry using complex geometries - a review. *Journal of Texture Studies*, 34, 1, 1-20, ISSN 1745-4603
- Dihoru, L. V.; Smith, L. N. & German R. M. (2000). Experimental analysis and neural network modeling of the rheological behaviour of powder injection moulding feedstocks formed with bimodal powder mixtures. *Powder Metallurgy*, 43, 1, 31-36, ISSN 0032-5899
- Drzal, P. L. & Shull, K. R. (2005). Elasticity, fracture and thermo-reversible gelation of highly filled physical gels. *The European Physical Journal E*, 17, 4, 477-483, ISSN 1292-895X
- Dvorak, P.; Barriere, T. & Gelin, J. C. (2005). Jetting in metal injection moulding of 316L stainless steel. *Powder Metallurgy*, 48, 3, 254-260, ISSN 0032-5899
- German, R. M. (1990). Powder injection moulding. *Metal Powder Industries Federation*, Princeton, ISBN 978-091-840-495-4

- González-Gutiérrez, J.; Stringari, G. B. & Emri, I. (2012). Powder injection molding of metal and ceramic parts. *Some Critical Issues for Injection Molding*, Dr. Jian Wang, 3, 65-85, ISBN 978-953-510-297-7
- Hausnerova, B. (2011). Powder injection moulding – an alternative processing method for automotive items. *New Trends and Developments in Automotive System Engineering*, Prof. Marcello Chiaberge, 7, 129-143, ISBN 978-953-307-517-4
- Hausnerová, B., Saha, P. & Kubat, J. (1999). Capillary flow of hard-metal carbide powder compounds. *International Polymer Processing*, 14, 3, 254- 260, ISSN 0930-777X
- Hausnerova, B.; Filip, P.; Jiranek, L. & Saha, P. (2011). Phase separation of highly filled powder/polymer compounds. *4th WSEAS International Conference on Materials Science*, Catania, Italy, ISBN 978-1-618-040-478-9
- Hausnerova, B.; Saha, P.; Kubat, J.; Kitano, T. & Becker, J. (2000). Rheological behaviour of hard-metal carbide powder suspensions at high shear rates. *Journal of Polymer Engineering*, 20, 4, 237-265, ISSN 0250-8079
- Hausnerova, B.; Sedlacek, T.; Slezak, R. & Saha, P. (2006). *Rheologica, Acta*, 45, 3, 290-296, ISSN 1435-1528.
- Honek, T.; Hausnerova, B. & Saha, P. (2005). Relative viscosity models and their application to capillary flow data of highly filled hard-metal carbide powder compounds. *Polymer Composites*, 26, 1, 29-36, ISSN 0272-8397
- Horvat, M. A.; Emin, M. A.; Hochstein, B.; Willenbacher, N. & Schechmann, H. P. (2013). Multiple-step slit die rheometer for rheological characterization of extruded starch melts. *Journal of Food Engineering*, 116, 2, 398-403
- Isayev, A. I. & Fan, X. (1994). Steady and oscillatory flows of silicon-polypropylene ceramic compounds. *Journal of Material Science*, 29, 2931-2938, ISSN 1573-4803
- Isayev, A. I. (1987). Rheology and Injection Moulding of Ceramic-Filled Materials. *Advances in Ceramics*, 21, 601-613
- Jenni M., Schimmer L., Zauner R., Stampfl J. & Morris J. (2008). Quantitative study of powder binder of feedstocks. *PIM International*, 2, 4, 50-55
- Johnson, J. L. & German, R. M. (2003). PIM materials. *Advanced materials & processes*, 35-39
- Kalyon, D. M. & Yilmazer, U. (1990). Rheological behaviour of highly filled suspensions which exhibit slip at the wall. *Highly Filled Material Institute*, 241-273

- Kalyon, D. M. (1993). Review of factors affecting the continuous processing and manufacturability of highly filled suspensions. *Journal of Material Processing & Manufacturing Science*, 2, 159-184, ISSN 1062-0656
- Lame, O.; Bellet, D.; Di Michiel, M. & Bouvard, D. (2003). In situ microtomography investigation of metal powder compacts during sintering. *Nuclear Instruments and Methods in Physics Research B*, 200, 287-294, ISSN 0168-583X
- Martin, P. J. & Wilson, D. I. (2005). A Critical assessment of the Jastrzebski interface condition or the capillary flow of pastes, foams and polymers. *Chemical Engineering Science*, 60, 2, 493-502
- Nickerson, C. S. & Kornfield, J. A. (2005). A "cleat" geometry for suppressing wall slip. *Journal of Rheology*, 49, 4, 865, ISSN 0148-6055
- Nickerson, CH. S. *Engineering the mechanical properties of ocular tissues* [online]. 2005, [cit. 2013-04-05]. <[http://thesis.library.caltech.edu/974/7/CSN\\_entire\\_thesis.pdf](http://thesis.library.caltech.edu/974/7/CSN_entire_thesis.pdf)>
- Palcevskis, E.; Faitelson, L. & Jakobsons, E. (2005). Rheology of organodispersions of Alumina nanopowders used in producing articles from engineering ceramics. *Mechanics of Composite Materials*, 41, 3, 255-265, ISSN 1573-8922
- Poslinski, A. J.; Ryan, M. E. & Gupta, R. K. (1988). Rheological behaviour of filled polymeric systems, I. Yield stress and shear-thinning effects. *Journal of Rheology*, 32, 7, 1, 703-735, ISSN 0148-6055
- Rothon, R. N. (2003). Particulate-filled polymer composites, 2nd edition. *Smithers Rapra Technology Limited*, Shropshire, United Kingdom, 29-33, ISBN 9781859573822
- Steffe, J. F. (1996). Rheological methods in food process engineering, second ed. *Freeman Press*, 418
- Thornagel, M. (2009). MIM-simulation: A virtual study on phase separation. *Proceedings of EURO PM 2009*, 2, 135-140, ISBN 978-189-907-207-1
- Thornagel, M. (2009). MIM-Simulation: A virtual study on phase separation. *Proceedings of EURO PM2009 Congress*, Shrewsbury, European Powder Metallurgy Association, 2, 135-140
- Williams, N. (2009). Fraunhofer IFAM: A commitment to industry oriented research helps drive MIM product development. *PIM International*, 3, 3, 51-56, ISSN 1753-1497
- Yaras, P.; Kalyon, D. M. & Yilmazer, U. (1994). Flow instabilities in capillary flow of concentrated suspensions. *Rheologica Acta*, 33, 1, 48-59, ISSN 1435-1528

- Yilmazer, U. & Kalyon, D. M. (1989). Slip effects in capillary and parallel disk torsional flows of highly filled suspensions. *Journal of Reology*, 33, 8, ISSN 0148-6055
- Yilmazer, U.; Gogos, C. G. & Kalyon, D. M. (1989). Mat formation and unstable flows of highly filled suspensions in capillaries and continuous processors. *Polymer Composites*, 10, 4, 242-249, ISSN 0272-8397
- Yoshimura, A. & Prud'homme, R. K. (1988). Wall slip corrections for Couette and parallel disk viscometers. *Journal of Rheology*. 32, 1, 53-67, ISSN 0148-6055

## LIST OF ABBREVIATIONS

BASF	Baden Aniline and Soda Factory
C	carbon
CIM	ceramic injection moulding
Cr	chrome
Cu	copper
<i>D</i>	capillary diameter
DSC	differential scanning calorimetry
EDX	energy dispersive X-ray
Fe	iron
<i>H</i>	height of flow channel
IFAM	Institute for Manufacturing Technology and Advanced Materials
<i>L</i>	length of capillary/flow channel
MIM	metal injection moulding
Mn	manganese
Mo	molybdenum
<i>n</i>	index of non-Newtonian behaviour
Ni	nickel
PIM	powder injection moulding
rpm	rotations per minute
SEM	scanning electron microscopy
Si	silicon
<i>W</i>	width of flow channel



## LIST OF FIGURES

Fig. 1. Schematic representation of PIM (Berginc et al., 2007) .....	12
Fig. 2. (A) Micrograph of feedstock material showing metallic particles surrounded by polymeric binder, (B) Pellets of commercially available feedstock material Catamold® by BASF (Gonzalez-Gutierrez et al., 2011).....	13
Fig. 3. Schematic representation of bimodal and monomodal molecular mass distribution in polymeric materials (Gonzalez-Gutierrez et al., 2011).....	17
Fig. 4. Flow pattern of highly filled polymer material across the channel causing powder - binder separation (Thornagel, 2009).....	20
Fig. 5. Detail of separated polymer-rich area (Hausnerova,2011).....	21
Fig. 6. New design of a testing mould (Hausnerova et al., 2011).....	22
Fig. 7. Apparent viscosity versus shear rate obtained with capillaries of L/D ratio of 57.6 (Kalyon, Yilmazer,1990).....	25
Fig. 8. Apparent shear rate versus reciprocal of capillary diameter, 1/D, for a suspension consisting of 76.5 % by volume solids in capillary flow (Kalyon, 1993) .....	26
Fig. 9. Viscosity vs. shear stress for a printing ink, measured in a parallel-plate geometry with smooth and roughened plates (Barnes, 1995).....	27
Fig. 10. Schematic representation of shear stress and velocity profile in capillary flow with apparent wall slip ( Kalyon, Yilmazer, 1990) .....	30
Fig. 11. Representation of the flow field found in a wide-gap concentric cylinder geometry with slip at both the inner and outer walls, for either the outer or inner rotating (Barnes, 1995).....	31
Fig. 12. Schematic representation of the velocity field in a sample experiencing shear deformation between parallel plates (A) when the no-slip boundary condition holds and (B) when it is violated (Nickerson, 2005).....	32
Fig. 13. Schematic representation of two cleated fixtures placed opposite each other. Sample motion penetrates only a short distance $\delta$ into the cleat array (Nickerson, 2005).....	34
Fig. 14. Scheme of measuring device with representation of pressure ( $p_1 - p_6$ ) and temperature transducers (T1, T2) and individual temperature zones (1, 2, 3 – extruder; 4 – slit die; 5 – movable valve).....	40
Fig. 15. Corrosion and strength attributes of the common PIM stainless steels (according to Johnson, German; 2003).....	41



- Fig. 16. Representation of slit die geometry with parameters (15/1/100) mm and roughened surface..... 43
- Fig. 17. Shear stress as a function of shear rate for PolyMIM 17-4PH feedstock extruded through smooth and roughened slit die with parameters (15/1/100) mm. The position of movable valve was (A) open, (B) half-closed and (C) closed..... 49
- Fig. 18. Shear stress as a function of shear rate for PolyMIM 17-4PH feedstock extruded through smooth and roughened slit die with parameters (10/0.5/100) mm. The position of movable valve was (A) open, (B) half-closed and (C) closed..... 50
- Fig. 19. Shear stress as a function of shear rate for PolyMIM 316L feedstock extruded through smooth and roughened slit die with parameters (15/1/100) mm and open position of movable valve..... 51
- Fig. 20. Shear stress as a function of shear rate for Catamold 316L feedstock extruded through smooth and roughened slit die with parameters (10/0.5/100) mm and open position of movable valve..... 52
- Fig. 21. The influence of slit die parameters on the rheological behaviour of PolyMIM 17-4PH feedstock for (A) smooth or (B) roughened surface slit die ..... 53
- Fig. 22. The influence of slit die parameters on the rheological behaviour of PolyMIM 316L feedstock for (A) smooth or (B) roughened surface slit die..... 53
- Fig. 23. Influence of the powder composition on the rheological behaviour of PolyMIM 17-4PH and PolyMIM 316L feedstocks for (A) smooth or (B) roughened slit die.... 54
- Fig. 24. Shear stress as a function of shear rate for Catamold 316L feedstock extruded through smooth and roughened slit die with parameters (15/1/100) mm and open position of movable valve..... 55
- Fig. 25. SEM images of polyMIM 17-4PH samples extruded through smooth and roughened slit die with (10/0.5/100) mm parameters at speeds (A) 3 rpm (B) 5 rpm (C) 10 rpm (D) 15 rpm (magnification 200x)..... 59
- Fig. 26. SEM images of polyMIM 17-4PH samples extruded through smooth and roughened slit die with (10/0.5/100) mm parameters at speeds (A) 3 rpm (B) 5 rpm (C) 10 rpm (D) 15 rpm (magnification 500x)..... 60
- Fig. 27. Surface analysis of PolyMIM 17-4PH samples extruded through smooth (left) and roughened (right) (10/0.5/100) mm slit die at speed 3 rpm ..... 61
- Fig. 28. Surface analysis of PolyMIM 17-4PH samples extruded through smooth (left) and roughened (right) (10/0.5/100) mm slit die at speed 5 rpm ..... 62

---

Fig. 29. Surface analysis of PolyMIM 17-4PH samples extruded through smooth (left) and roughened (right) (10/0.5/100) mm slit die at speed 10 rpm ..... 62

Fig. 30. Surface analysis of PolyMIM 17-4PH samples extruded through smooth (left) and roughened (right) (10/0.5/100) mm slit die at speed 15 rpm ..... 63

**LIST OF TABLES**

Table 1 Material characteristic of PolyMIM 17-4PH .....	36
Table 2 Material characteristic of PolyMIM 316L .....	37
Table 3 Material characteristic of Catamold 316L .....	37
Table 4 Material characteristic of Embemold 17-4PH .....	38
Table 5 The roughness parameters of smooth and roughened (10/0.5/100) mm slit die channels in longitudinal direction.....	44
Table 6 The roughness parameters of smooth and roughened (10/0.5/100) mm slit die channels in transverse direction.....	45
Table 7 The roughness parameters of smooth and roughened (15/1/100) mm slit die channels in longitudinal direction.....	45
Table 8 The roughness parameters of smooth and roughened (15/1/100) mm slit die channels in transverse direction.....	46
Table 9 Indexes of non-newtonian behaviour calculated for the individual materials .....	57

